

Capacity and Delay Analysis of Next-Generation Passive Optical Networks (NG-PONs)

Frank Aurzada, Michael Scheutzow, Martin Reisslein, Navid Ghazisaidi, and Martin Maier

Abstract

Building on the Ethernet Passive Optical Network (EPON) and Gigabit PON (GPON) standards, Next-Generation (NG) PONs (*i*) provide increased data rates, split ratios, wavelengths counts, and fiber lengths, as well as (*ii*) allow for all-optical integration of access and metro networks. In this paper we provide a comprehensive probabilistic analysis of the capacity (maximum mean packet throughput) and packet delay of subnetworks that can be used to form NG-PONs. Our analysis can cover a wide range of NG-PONs through taking the minimum capacity of the subnetworks making up the NG-PON and weighing the packet delays of the subnetworks. Our numerical and simulation results indicate that our analysis quite accurately characterizes the throughput-delay performance of EPON/GPON tree networks, including networks upgraded with higher data rates and wavelength counts. Our analysis also characterizes the trade-offs and bottlenecks when integrating EPON/GPON tree networks across a metro area with a ring, a Passive Star Coupler (PSC), or an Arrayed Waveguide Grating (AWG) for uniform and non-uniform traffic. To the best of our knowledge, the presented analysis is the first to consider multiple PONs interconnected via a metro network.

I. INTRODUCTION

The Passive Optical Network (PON) is one of the most widely deployed access networks due to its unique benefits, including transparency against data rate and signal format. The two major state-of-the-art PON standards IEEE 802.3ah Ethernet PON (EPON) and ITU-T G.984 Gigabit PON (GPON) consist both of a single upstream wavelength channel and a separate single downstream wavelength channel, whereby both channels are operated with time division multiplexing (TDM). EPON and GPON are expected to coexist for the foreseeable future as they evolve into Next-Generation PONs (NG-PONs) [1], [2], [3]. NG-PONs are mainly envisioned to (*i*) achieve higher performance parameters, e.g., higher bandwidth per subscriber, increased split ratio, and extended maximum reach, than current EPON/GPON architectures [4], and (*ii*) broaden EPON/GPON functionalities to include, for instance, the consolidation of optical access, metro, and backhaul networks, the support of topologies other than conventional tree structures, and protection [5]. Throughout, network operators are seeking NG-PON solutions that can transparently coexist with legacy PONs on the existing fiber infrastructure and enable gradual upgrades in order to avoid costly and time consuming network modifications and stay flexible for further evolution paths [1].

F. Aurzada and M. Scheutzow are with the Department of Mathematics, Technical University Berlin, 10623 Berlin, Germany, Email: {aurzada, ms}@math.tu-berlin.de

M. Reisslein is with the Department of Electrical Engineering, Arizona State University, Tempe, Arizona 85287-5706, USA, Email: reisslein@asu.edu

N. Ghazisaidi and M. Maier are with the Optical Zeitgeist Laboratory, INRS, University of Québec, Montréal, QC, H5A 1K6, Canada, Email: {navid,maier}@emt.inrs.ca

In this paper, we evaluate the capacity (maximum mean packet throughput) and packet delay of a wide range of NG-PONs through probabilistic analysis and verifying simulations. More specifically, we analyze the capacity and delay of various subnetworks from which NG-PONs can be formed, thus enabling analytical capacity and delay characterization for a wide range of NG-PONs built from the examined subnetworks. Two important applications for our analysis are: (A) The obtained results provide insight into the performance limitations of candidate NG-PON architectures and thus inform network operators seeking to upgrade their installed TDM PONs. (B) Neither IEEE 802.3ah EPON nor ITU-T G.984 GPON standardizes a specific dynamic bandwidth allocation (DBA) algorithm. The design of DBA algorithms is left to manufacturers which aim at equipping network operators with programmable DBA algorithms that adapt to new applications and business models and thus make PONs future-proof. Our capacity and delay analysis provides an upper throughput bound and a delay benchmark for gated service [6] which can be used to evaluate the throughput-delay performance of current and future DBA algorithms for NG-PONs.

This paper is structured as follows. In the following section, we review related work on the analysis of PON access and metro packet networks. In Section III we give overviews of the EPON and GPON access networks. In Section IV, we present NG-PONs that either (i) upgrade PONs or (ii) interconnect multiple PONs across a metropolitan area. We conduct the capacity and delay analysis of the subnetworks making up NG-PONs in Sections VI and VII. We first introduce the network model and then evaluate the capacity (maximum mean aggregate throughput). Subsequently, we analyze the packet delays. In Section VIII, we compare numerical throughput-delay results obtained from our analysis with simulations and illustrate the application of our capacity analysis to identify bottlenecks in NG-PONs. We briefly summarize our contributions in Section IX.

II. RELATED WORK

In this section we briefly review related work on the analysis of passive optical networks and metropolitan area networks. EPONs employ medium access control with an underlying polling structure [7], [8], [9], [10]. Building directly on the extensive literature on polling systems, see e.g., [11], Park et al. [12] derive a closed form delay expression for a single-channel EPON model with random independent switchover times. The EPON model with independent switchover times holds only when successive upstream transmissions are separated by a random time interval sufficiently large to “de-correlate” successive transmissions, which would significantly reduce bandwidth utilization in practice.

In an EPON, the service (upstream transmission) of an Optical Network Unit (ONU) follows immediately (separated by a guard time) after the upstream transmission of the preceding ONU to ensure high utilization. The switchover time is therefore generally highly dependent on the round-trip delays and the masking of the round-trip delays through the interleaving of upstream transmissions [6]. Subsequent analyses have strived to model these correlated transmissions and switchovers with increasing fidelity. In particular, EPONs with a static bandwidth allocation to the ONUs were analyzed in [13], [14] and

it was found that the static bandwidth allocation can meet delay constraints only at the expense of low network utilization. Packet delay analyses for single-channel EPONs with dynamic bandwidth allocation have been undertaken in [15], [16], [17], [18], [14], [19], [20]. A dynamic bandwidth allocation scheme with traffic prediction assuming a Gaussian prediction error distribution was analyzed in [21]. A grant estimation scheme was proposed and its delay savings analyzed in [22].

GPONs have received relatively less research interest than EPONs. To the best of our knowledge we conduct the first delay analysis of GPONs in this paper.

Similarly, WDM PONs have received relatively little research attention to date. The call-level performance of a WDM PON employing Optical Code Division Multiple Access was analyzed in [23]. To the best of our knowledge a packet-level analyses of WDM EPONs has so far only been attempted in [24, Section 2.4] where an offline scheduling WDM EPON was analyzed with the help of a two stage queue. In offline EPONs, also referred to as EPONs with interleaved polling with stop [10], the Optical Line Terminal (OLT) collects bandwidth requests from all ONUs before making bandwidth allocation decisions. An offline scheduling EPON was also considered in [25] where the stability limit (capacity) and packet delay were analyzed. In contrast, we analyze in this paper the capacity and packet delay for WDM PON channels that are integrated into an online scheduling PON, i.e., transmissions from the different ONUs are interleaved to mask propagation delays.

Metropolitan area networks have received significant attention over the past two decades. The capacity and delay performance of packet ring networks with a variety of MAC protocols has been analyzed in numerous studies, see e.g., [26], [27], [28], [29]. More recently, analyses of medium access and fairness mechanisms for the resilient packet ring have been undertaken, see for instance [30], [31]. The impact of fiber shortcuts in ring networks has been analyzed in [32]. Metropolitan star networks based on passive star couplers (see e.g., [33]) and arrayed waveguide gratings (see e.g., [34]) have been analyzed in isolation. In this paper, we analyze to the best of our knowledge for the first time a comprehensive NG-PON that interconnects multiple PONs via a metro network combining a ring and star networks.

III. OVERVIEW OF EPON AND GPON

While EPONs are deployed mostly in the Asia-Pacific region, GPONs are leading in the U.S. and Europe. Typically, both EPON and GPON have a physical tree topology with the Optical Line Terminal (OLT) at the root. The OLT connects through an optical splitter to multiple Optical Network Units (ONUs), also known as Optical Network Terminals (ONTs). Each ONU can serve a single or multiple subscribers. To facilitate DBA, both EPON and GPON use polling based on a *report/grant mechanism*. In each polling cycle, ONUs send their instantaneous upstream bandwidth demands through report messages to the OLT, which in turn dynamically allocates variable upstream transmission windows by sending a separate grant message to each ONU. EPON and GPON have some major and minor differences with respect to polling timing structure, line rate, reach, split ratio, guard time, protocol overhead, and bandwidth efficiency [1].

A. Major Differences

The EPON is a symmetric network providing a data rate of 1 Gb/s in both upstream and downstream directions. It provides a reach between OLT and ONUs of up to 20 km for a split ratio as high as 1:64. The EPON has variable-length polling cycles based on the bandwidth demands, which are signalled with the multipoint control protocol (MPCP). The ONU uses the MPCP REPORT message to report bandwidth requirements of up to eight priority queues to the OLT. The OLT passes received REPORT messages to its DBA algorithm module to calculate the upstream transmission schedule. Then, the OLT issues upstream transmission grants by transmitting a GATE message to each ONU. Each GATE message supports up to four transmission grants, each specifying the start time and length of the transmission window. The transmission window may comprise multiple Ethernet frames, whereby EPON does not allow for fragmentation. EPON carries Ethernet frames natively, i.e., without encapsulation.

The GPON offers several combinations of upstream/downstream data rates with a maximum symmetric data rate of 2.488 Gb/s. GPON supports up to 60 km reach, for a maximum split ratio of 1:128. Both upstream and downstream transmissions are based on a periodically recurring time structure with a fixed frame length of $\delta = 125 \mu\text{s}$. Each upstream frame contains dynamic bandwidth report (DBRu) fields. Each downstream frame contains a physical control block (PCBd), which includes a bandwidth map (BWmap) field specifying the ONU upstream transmission grants. Unlike the EPON, the GPON deploys the GPON encapsulation method (GEM) involving a 5-byte GEM header and allows for Ethernet frame fragmentation. Two DBA methods are defined for GPON: (i) status-reporting DBA based on ONU reports via the DBRu field, and (ii) non-status-reporting DBA based on traffic monitoring at the OLT. Recent GPON research has focused on the design and evaluation of status-reporting DBA algorithms [35], [36], [37].

B. Minor Differences

EPON uses various guard times between two neighboring transmission windows, e.g., the laser on-off time. In GPON, additional fields are used in each upstream and downstream frame, e.g., the physical layer operation, administration, and maintenance (PLOAM) field. The impact of the various types of guard times and overhead fields on the bandwidth efficiency of both EPON and GPON was thoroughly investigated in [38], [39], and we consequently neglect all overheads in our analysis to uncover the fundamental underlying performance characteristics due to the different polling timing structures, i.e., variable-length cycles in EPON and fixed-length frames in GPON.

IV. NG-PONs

NG-PONs are PONs that provide (i) higher data rates, larger counts of wavelength channels, longer ranges, and/or higher split ratios, as well as (ii) broader functionalities than current EPON and GPON networks, as explained next.

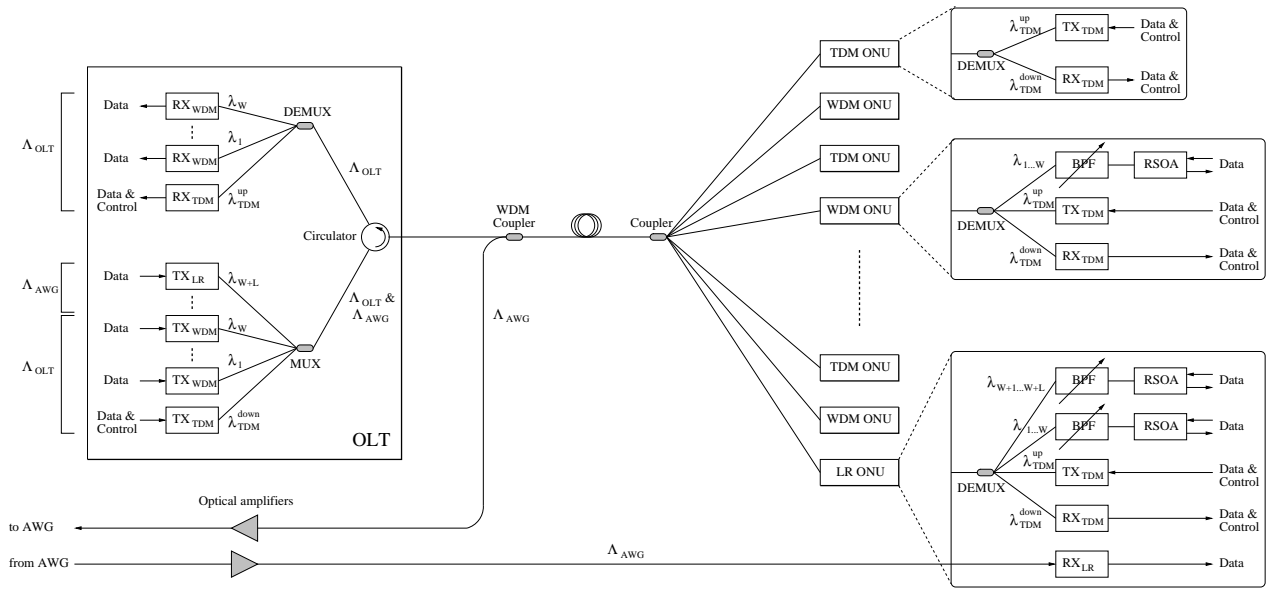


Fig. 1. Evolutionary upgrade of legacy TDM ONUs to WDM ONUs and long-reach ONUs (LR ONUs) and their coexistence on the same NG-PON fiber infrastructure.

A. High-speed TDM PON

Higher speeds are needed to support emerging bandwidth-hungry applications, e.g., high-definition television and video on demand, and to provide sufficient capacity as backhauls of next-generation IEEE 802.11n wireless LANs with a throughput of 100 Mb/s or higher per device [4]. For both EPON and GPON, standardization efforts have begun to specify symmetric or asymmetric data rates of up to 10 Gb/s [1]. DBA algorithms for EPON, GPON, and high-speed TDM PON are compared in [39].

B. WDM PON

Different forms of WDM PONs have been actively studied as a component of NG-PON [5]. In a wavelength-routing WDM PON, each ONU is assigned a dedicated pair of wavelength channels for upstream and downstream transmission, which brings some advantages, but requires replacing the power splitter in installed TDM PONs with a wavelength demultiplexer. According to [1], a more practical approach towards WDM PONs is to leave the existing power-splitting PON infrastructure in place and to select wavelengths at each ONU using a bandpass filter (BPF) with a small insertion loss of 1 dB. To ensure that WDM enhanced ONUs, operating on additional wavelengths, can be installed on legacy TDM PON infrastructures, the conventional TDM ONUs may be equipped with wavelength blocking filters which let only the legacy TDM wavelength pass.

The MPCP can be extended to support a wide range of possible WDM ONU structures by exploiting the reserved bits of GATE, REPORT, and other MPCP messages [40]. Similar WDM extensions can be designed for GPON by exploiting the reserved bits in BWmap, DBRu, and other fields of each time

frame. In WDM PONs, so-called colorless (i.e., wavelength-independent) ONUs should be deployed such that only a single type of WDM ONU is required, thereby greatly simplifying inventory, maintenance, and installation [1]. A promising approach toward realizing low-cost colorless ONUs is to use a reflective semiconductor optical amplifier (RSOA) at the ONU to perform remote modulation, amplification, and reflection of an optical seed signal sent by the OLT. The optical seed signal can be either (i) a modulated signal carrying downstream data, or (ii) an unmodulated *empty carrier*. In the former case, the ONU reuses the modulated carrier by means of *remodulation* techniques, e.g., FSK for downstream and OOK for upstream [5].

C. Long-reach PON

Long-reach PONs increase the range and split ratio of conventional TDM and WDM PONs significantly [41], [42], [43], [44]. State-of-the-art long-reach PONs are able to have a total length of 100 km potentially supporting 17 power-splitting TDM PONs, each operating at a different pair of upstream and downstream wavelength channels and serving up to 256 colorless ONUs, translating into a total of 4352 colorless ONUs [45]. Importantly, such long-reach PON technologies allow for the integration of optical access and metro networks, i.e., broaden the functionality of PONs. This broadened PON functionality offers major cost savings by reducing the number of required optical-electrical-optical (OEO) conversions, at the expense of optical amplifiers required to compensate for propagation and splitting losses [44].

D. Migration Toward Integrated Access-Metro Networks

To provide backward compatibility with legacy infrastructure, current TDM PONs are expected to evolve toward NG-PONs in a pay-as-you-grow manner. Fig. 1 depicts a tree network architecture for an evolutionary upgrade from legacy TDM ONUs to WDM ONUs and long-reach ONUs (LR ONUs), which was originally proposed, but not formally analyzed, in [46]. We briefly review this tree architecture here and incorporate it as a subnetwork for building an NG-PON in our original capacity and delay analysis.

1) *OLT Architecture*: The OLT is equipped with an array of fixed-tuned transmitters (TX) for transmission of control and data in the downstream direction and a separate array of fixed-tuned receivers (RX) for reception of control and data in the upstream direction. Specifically, the OLT deploys one TX_{TDM} and one RX_{TDM} to send and receive control and data on the downstream wavelength channel $\lambda_{\text{TDM}}^{\text{down}}$ and upstream wavelength channel $\lambda_{\text{TDM}}^{\text{up}}$, respectively, of the original TDM EPON network (note that $\lambda_{\text{TDM}}^{\text{down}}$ and $\lambda_{\text{TDM}}^{\text{up}}$ are two different wavelengths). In addition, the OLT may deploy arrays of fixed-tuned transmitters and receivers for data transmission only (no control). More precisely, the OLT may deploy W fixed-tuned transmitters and W fixed-tuned receivers, where $W \geq 0$. These W transmitters and receivers operate on W different wavelength channels $\lambda_1, \dots, \lambda_W$ (note that there are exactly W wavelengths which are alternately used for downstream transmission and upstream transmission, as described in greater detail in Section V). The two wavelength channels $\lambda_{\text{TDM}}^{\text{down}}$ and $\lambda_{\text{TDM}}^{\text{up}}$ together with the W wavelength channels

make up the waveband Λ_{OLT} , whose $2 + W$ wavelengths allow for direct optical communication between OLT and ONUs belonging to the same EPON tree network.

For optical communication between ONUs belonging to different EPON tree networks, the OLT uses additional L fixed-tuned transmitters TX_{LR} (but no additional receivers), where $L \geq 0$. These L transmitters operate on L separate wavelength channels $\lambda_{W+1}, \dots, \lambda_{W+L}$, which make up the waveband Λ_{AWG} . Recall that these L wavelengths do not necessarily need to be adjacent. These wavelengths are used to all-optically interconnect different EPON tree networks with suitable traffic demands (defined shortly).

In the downstream direction, the two wavebands Λ_{OLT} and Λ_{AWG} are combined via a multiplexer (MUX) and guided by the circulator toward the coupler which equally distributes both wavebands among all N ONUs. In the upstream direction, the WDM coupler in front of the OLT is used to separate the two wavebands from each other; the waveband Λ_{OLT} is forwarded to the circulator which guides it onwards to the demultiplexer (DEMUX) that in turn guides each wavelength channel to a different fixed-tuned receiver. Whereas the waveband Λ_{AWG} is not terminated at the OLT (therefore no need for receivers at the OLT) and optically bypasses the OLT, possibly amplified, on its way to the AWG of the star subnetwork, as explained in Section IV-F1.

2) *ONU Architectures*: There are three different types of ONU architecture:

- **TDM ONU**: The TDM ONU is identical to an ONU of a conventional TDM EPON network. It is equipped with a single fixed-tuned transmitter TX_{TDM} and a single fixed-tuned receiver RX_{TDM} operating on the upstream wavelength channel $\lambda_{\text{TDM}}^{\text{up}}$ and downstream wavelength channel $\lambda_{\text{TDM}}^{\text{down}}$, respectively. Each wavelength channel in either direction is used to send both data and control. The DEMUX is used to separate the two wavelength channels.
- **WDM ONU**: The WDM ONU is more involved than the TDM ONU in that it additionally allows to send and receive data on any other wavelength channel $\lambda_1, \dots, \lambda_W$ of waveband Λ_{OLT} . To do so, the WDM ONU deploys an extra bandpass filter (BPF) and reflective semiconductor optical amplifier (RSOA). The BPF can be tuned to any of the wavelengths $\lambda_1, \dots, \lambda_W$ and blocks all but one wavelength λ_i , $i = 1, \dots, W$. The wavelength λ_i passing the BPF is forwarded to the RSOA. At any given time, the RSOA can be in either one of the following two operation modes: (i) reception of downstream data on λ_i coming from the OLT, or (ii) transmission of upstream data on λ_i originating from the WDM ONU, as explained in greater detail in Section V-A.
- **LR ONU**: The LR ONU builds on the WDM ONU. Similar to the WDM ONU, the LR ONU has a BPF that is tunable over the wavelengths $\lambda_1, \dots, \lambda_W$. In addition, the LR ONU has a RSOA and BPF tunable over wavelengths $\lambda_{W+1}, \dots, \lambda_{W+L}$, i.e., this second BPF is tunable over the waveband Λ_{AWG} . As a result, the LR ONU can send and receive data also on any wavelength channel of waveband Λ_{AWG} , which optically bypasses the OLT and allows for direct optical communication with ONUs residing in different EPON tree networks. Apart from two BPFs and two RSOAs, the LR

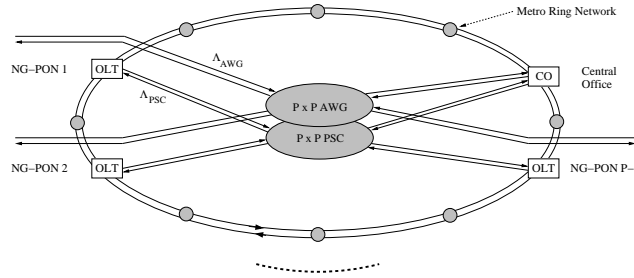


Fig. 2. Integration of NG-PONs and remote central office using the AWG as a wavelength router and a bidirectional metro ring and star subnetwork for enhanced resilience.

ONU deploys an additional multiwavelength receiver RX_{LR} that is able to simultaneously receive data on all L wavelength channels of waveband Λ_{AWG} coming from the AWG of the star subnetwork, possibly amplified.

Note that an EPON tree network may accommodate any combination of N_T TDM ONUs, N_W WDM ONUs, and N_L LR ONUs, whereby $0 \leq N_T, N_W, N_L \leq N$ and $N_T + N_W + N_L = N$.

As illustrated in Fig. 2, the OLTs of $P - 1$, $P > 2$, NG-PON access networks (shown in Fig. 1) and H remote COs in a metro area may be interconnected with any combination of (i) a bidirectional metro ring network, e.g., Gigabit Ethernet or RPR, with N_r ring nodes, (ii) a wavelength-broadcasting $P \times P$ passive star coupler (PSC) with Λ_{PSC} wavelength channels, comprising P data wavelength channels (one assigned to each OLT and CO) and one control wavelength for conducting a reservation based medium access control, and (iii) an AWG employed as a $P \times P$ wavelength router. Importantly, the AWG provides any-to-any optical single-hop connections among the $P - 1$ NG-PONs and the CO, i.e., integrates access and metro networks into one single-hop optical network, and is therefore the key to vastly improved performance as demonstrated in Section VIII. In addition, the AWG allows for spatial reuse of all Λ_{AWG} wavelengths at each AWG port, resulting in a significantly increased capacity. Using two or more of these interconnections options in parallel enhances network resilience. In the following, the interconnection network segments are described at length in separate subsections.

E. Metro Ring Network

The metro ring network, e.g., Gigabit Ethernet or RPR, interconnects multiple EPON tree networks among each other as well as to the Internet and server farms. The ring network consists of P central offices (COs) and N_r ring nodes equally spaced on the ring ($P = 4$ and $N_r = 8$ in Fig. 2). The CO in the upper right corner of the figure is assumed to be attached to the Internet and a number of servers via a common router. We refer to this $H = 1$ CO as the *hotspot* CO. Each of the other $P - H = 3$ COs is collocated with the optical line terminal (OLT) that belongs to the attached EPON tree network.

In case of an RPR metro ring network, the ring is a optical dual-fiber bidirectional ring network, where each fiber carries a single wavelength channel (i.e., no wavelength division multiplexing [WDM]). Each

RPR ring node and CO is equipped with two pairs of fixed-tuned transmitter and fixed-tuned receiver, one for each fiber ring. Each ring node and CO has separate (electrical) transit and station queues for either ring. Specifically, for each ring, a node has one transit queue for in-transit traffic, one transmission queue for locally generated data packets, and one reception queue for packets destined for the local node. In-transit ring traffic is given priority over station traffic so that in-transit packets are not lost due to buffer overflow. Thus, the transit path is lossless, i.e., a packet put on the ring is not dropped at downstream nodes. On the downside, however, a node ready to send data has to wait for the transit path to be empty before it can send data. Nodes perform destination stripping, i.e., the destination node of a given packet takes the packet off the ring, to let nodes downstream from the destination node use the ring for packet transmission. Typically, nodes deploy shortest path routing, i.e., a source node selects the fiber ring that provides the shortest path to the destination node in terms of number of traversed intermediate nodes (hops).

F. Star Subnetwork

The P COs of the RPR ring network are interconnected via a single-hop WDM star subnetwork whose hub is based on a $P \times P$ passive star coupler (PSC) in parallel with a $P \times P$ arrayed waveguide grating (AWG). The PSC is a wavelength-broadcasting device, i.e., each wavelength arriving on any PSC input port is equally distributed to all PSC output ports. In contrast, the AWG is a wavelength-routing device. The AWG allows for the spatial reuse of all wavelength channels at each AWG port. Fig. 2 illustrates spatial wavelength reuse for an 8×8 AWG ($P = 8$) and eight wavelengths $\lambda_1, \dots, \lambda_8$. Observe that the same wavelength channel can be simultaneously deployed at two (and more) AWG input ports without resulting in channel collisions at the AWG output ports. For instance, wavelength λ_4 incident on input ports 1 and 2 is routed to different output ports 4 and 5, respectively. The wavelength-routing characteristics of the AWG have the following two implications:

- Due to the fact that the AWG routes wavelengths arriving at a given input port independently from all other AWG input ports, no network-wide scheduling but only local scheduling at each AWG input port is necessary to avoid channel collisions on the AWG.
- Note that in Fig. 2 each AWG input port reaches a given AWG output port on a different wavelength channel. Consequently, with full spatial wavelength reuse, eight different wavelengths arrive at each AWG output port simultaneously. To avoid receiver collisions, each AWG output port must be equipped with a receiver operating on all eight wavelengths. (A receiver collision occurs if none of the destination node's receivers is tuned to the wavelength on which data arrives.)

The one-way end-to-end propagation delay of the star subnetwork equals τ_{star} . Each CO is attached to a separate input/output port of the $P \times P$ AWG and $P \times P$ PSC by means of two pairs of counterdirectional fiber links. Each fiber going to and coming from the AWG carries $\Lambda_{\text{AWG}} = L$ wavelength channels,

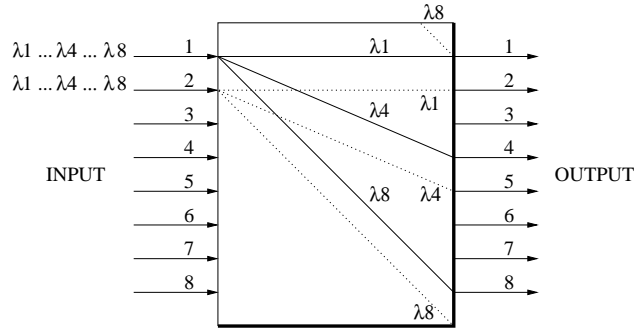


Fig. 3. Wavelength routing of an 8×8 AWG.

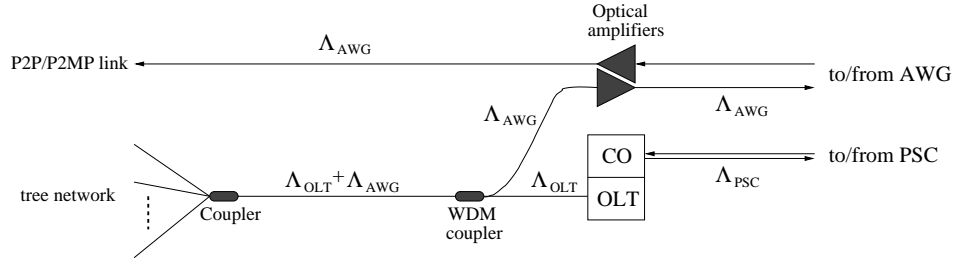


Fig. 4. Optical bypassing of collocated OLT and CO.

whereby L denotes an integer number of wavelengths that do not necessarily need to be adjacent. Each fiber going to and coming from the PSC carries $\Lambda_{\text{PSC}} = 1 + h + (P - 1)$ wavelength channels, consisting of one control channel λ_c , $1 \leq h \leq P - 1$ dedicated home channels for the hotspot CO, and $(P - 1)$ dedicated home channels, one for each of the remaining $(P - 1)$ COs. The home channels are fixed assigned to the respective COs for data reception. Data destined for a certain CO is sent on its corresponding home channel(s).

Each CO has one transmitter and one receiver fixed tuned to the control channel λ_c . In addition, for data reception, each CO (except the hotspot CO) has a single receiver fixed-tuned to its PSC home channel. The hotspot CO is equipped with $1 \leq h \leq P - 1$ receivers fixed-tuned to its h PSC home channels. For data transmission on the PSC, each CO (except the hotspot CO) deploys a single transmitter that can be tuned over the $(P - 1) + h$ home channels of the COs. The hotspot CO deploys h tunable transmitters whose tuning range covers the home channels of the remaining $(P - 1)$ COs as well as the Λ_{AWG} wavelength channels. Thus, among all COs only the hotspot CO is able to send data on the Λ_{AWG} wavelength channels. Unlike the remaining COs, the hotspot CO is equipped with an additional multiwavelength receiver operating on all Λ_{AWG} wavelength channels. Hence, only the hotspot CO is able to receive data on the Λ_{AWG} wavelength channels. Note that the remaining COs are unable to access the Λ_{AWG} wavelength channels, which optically bypass these COs and their collocated OLTs.

1) *Optical Bypassing*: In the following, we describe how the Λ_{AWG} wavelength channels optically bypass the OLT of Fig. 1 as well as the collocated CO of Fig. 2. Fig. 4 depicts the interconnection of a given EPON tree network and the star subnetwork, illustrating the optical bypassing of the collocated OLT and CO. Note that the Λ_{AWG} wavelength channels are carried on the tree network only in the upstream direction, while in the downstream direction they are carried on a separate point-to-point (p2p) or point-to-multipoint (p2mp) fiber link. A p2p fiber link connects a single LR ONU (as illustrated in Fig. 1) to the AWG of the star subnetwork, or more generally, a p2mp fiber link connects multiple LR ONUs (as in Fig. 2) to the AWG of the star subnetwork. As shown in Fig. 4, a WDM coupler is used on the tree network in front of the OLT to separate the Λ_{AWG} wavelength channels from the Λ_{OLT} wavelength channels and to guide the Λ_{AWG} wavelength channels directly onward to the AWG of the star subnetwork, optically amplified if necessary. In doing so, the Λ_{AWG} wavelength channels are able to optically bypass the CO and OLT without being electrically terminated. Similarly, the Λ_{AWG} wavelength channels coming from the AWG optically bypass both CO and OLT and directly travel on the p2p or p2mp link onward to the subset of attached single LR ONU or multiple LR ONUs, respectively. As a result, the LR ONU(s) as well as the hotspot CO that send and receive data on any of the Λ_{AWG} wavelength channels are able to communicate all-optically with each other in a single hop across the AWG of the star subnetwork.

V. OPERATION

In this section, we outline how the interconnection of the NG PONs across the metro area works. We first note that each CO performs store-and-forward transmission with OEO conversion for each packet traversing the CO, i.e., the packet must first be completely received before it can be transmitted onto the next subnetwork. Each ring node performs cut-through transmission for each packet traversing the node, i.e., the packet is received and forwarded on (ideally) a bit-by-bit basis.

Before explaining the details of the network operation, we briefly describe the operation of the RSOA used in the WDM ONU and LR ONU of Fig. 1, followed by reporting bandwidth requirements of ONUs, granting transmission windows to ONUs, dynamic bandwidth allocation, access control on ring and PSC, as well as considered traffic types.

A. RSOA

The RSOA has two different operating modes: (i) reception of downstream data sent by the OLT to the ONU, and (ii) transmission of upstream data generated by the ONU and destined for the OLT (on wavelengths $\lambda_1, \dots, \lambda_W$), or for an LR ONU residing in a different EPON tree network (on wavelengths $\lambda_{W+1}, \dots, \lambda_L$). The two modes are alternated on a time basis and at any given time the RSOA can be in either one of these two modes or in idle state (to be discussed shortly).

Fig. 5 illustrates the two operation modes (i) and (ii) of an RSOA and also explains the impact of reflection on the upstream data reception. Suppose that the OLT first sends downstream data during the

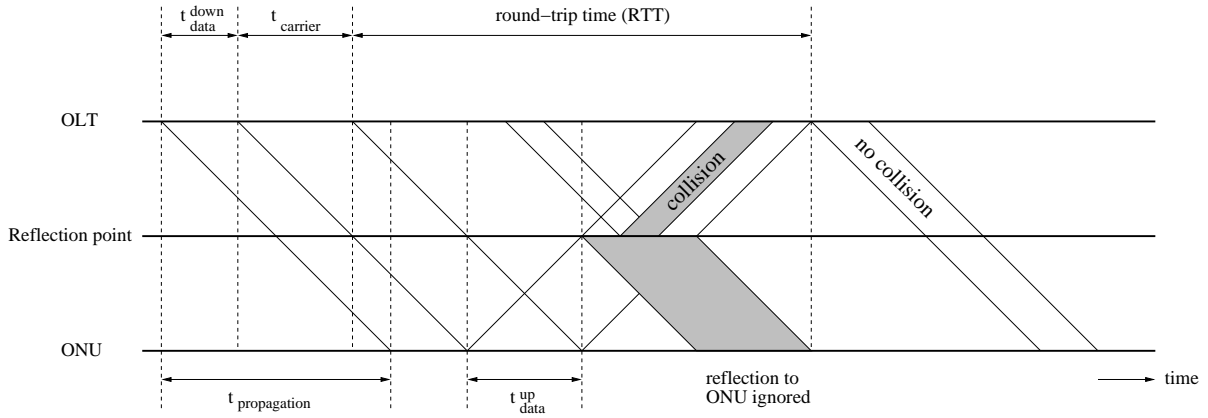


Fig. 5. RSOA operation modes subject to reflection.

time interval t_{data}^{down} using one of its fixed-tuned transmitters TX_{WDM} or TX_{LR} . After the propagation delay $t_{propagation}$, or briefly τ_T , the data arrives at the destination ONU.

The upstream data transmission from ONU to OLT is a bit more involved due to the fact that the RSOA does not have its own light source. As a consequence, the OLT has to generate light by using one of its WDM transmitters TX_{WDM} (in case of a WDM ONU or LR ONU) or one of its LR transmitters TX_{LR} (only in case of an LR ONU) and send it downstream to the ONU. We consider two approaches for supplying light to the RSOA: the empty carrier approach, and the reflection of downstream data signal approach. We first describe the empty carrier approach where a light carrier signal that does not carry any data is supplied to the RSOA for upstream data transmission. In Fig. 5, suppose that after transmitting its downstream data, the OLT sends the generated light to the ONU during the time period $t_{carrier}$, or briefly t_c , which can be of any arbitrary length. Note that this light does not convey any downstream data; it may be viewed as an “empty” carrier arriving after t_p at the ONU. The RSOA acts as a mirror and the ONU uses the carrier light reflected by the RSOA for sending its upstream data to the OLT during the time interval t_{data}^{up} . The upstream data transmission takes t_p to arrive at the OLT. Now, to guarantee that the upstream data is received by the OLT without collision, the OLT must not use the same wavelength for downstream data transmission until the upstream data is completely received by the OLT. In other words, after generating the light and sending it downstream to the ONU, the OLT has to wait for one round-trip time (RTT), i.e., $2\tau_T$, until it is allowed to use the same wavelength again for downstream data transmission.

To better understand this constraint, Fig. 5 illustrates the case where the OLT does not wait for one RTT and starts its next downstream data transmission before one RTT has elapsed. The second downstream data transmission might be reflected at a reflection point (e.g., splice or connector) somewhere between the OLT and ONU and interfere with the upstream data transmission of the ONU, resulting in a collision. Clearly, by deferring its next downstream data transmission by at least one RTT, the OLT can avoid any

collisions. However, note that while waiting for the wavelength to become available, the OLT may use the downstream wavelength channel $\lambda_{\text{TDM}}^{\text{down}}$ and the other WDM wavelength channels to send data to any (WDM, LR, and TDM) ONU. Also note that this restriction holds only for data but not for carrier sent in the downstream direction. For instance, in Fig. 5 the OLT might generate a second carrier on the same wavelength destined for a different ONU right after t_c , provided that the upstream data transmission of the second ONU does not overlap with the first one due to different propagation delays between OLT and the two ONUs. With the reflection of downstream data signal approach, the downstream data signal is used as carrier signal for upstream data transmission.

B. REPORT Message

Each ONU monitors traffic incoming from its attached users and classify it into one or more different traffic types. Specifically, each TDM ONU and each WDM ONU considers all incoming traffic the same and store it in a single first-in-first-out (FIFO) queue (for service differentiation we might later consider multiple FIFO queues, one for each traffic class). In each polling cycle, every TDM/WDM ONU sends its current bandwidth requirements (queue occupancy) in its assigned REPORT message to the OLT on wavelength channel $\lambda_{\text{TDM}}^{\text{up}}$. In contrast, each LR ONU splits incoming traffic into two different traffic types, using two separate FIFO queues. The first queue, which we call *OLT queue*, stores traffic to be sent on any of the Λ_{OLT} upstream wavelengths. The second queue, which we call *AWG queue*, stores traffic to be sent on one of the Λ_{AWG} wavelength channels (as discussed in more detail shortly). In each polling cycle, every LR ONU reports its current bandwidth requirements (queue occupancies) on both Λ_{OLT} and Λ_{AWG} in a single REPORT message to the OLT on $\lambda_{\text{TDM}}^{\text{up}}$. More precisely, an LR ONU writes its bandwidth requirements on Λ_{OLT} into the REPORT message, similar to a TDM or WDM ONU. In addition, an LR ONU writes its bandwidth requirements on Λ_{AWG} and the addresses of the corresponding destination ONUs into the REPORT message. Thus, the bandwidth requirements on Λ_{AWG} (including destination ONU address) ride piggyback on those on Λ_{OLT} within the same REPORT message.

C. GATE Message

After receiving the REPORT message(s), the OLT sends a GATE message to each ONU on the downstream wavelength channel $\lambda_{\text{TDM}}^{\text{down}}$. The GATE message contains one or two transmission grants, depending on the ONU type. Specifically, for a TDM ONU the GATE message contains a single grant that specifies the start time and duration of its allocated upstream TDM transmission window on wavelength channel $\lambda_{\text{TDM}}^{\text{up}}$. The TDM transmission window on $\lambda_{\text{TDM}}^{\text{up}}$ is also used by the TDM ONU to send its next REPORT message to the OLT. Conversely, for WDM ONUs and LR ONUs the GATE message contains two transmission grants, the TDM transmission window for $\lambda_{\text{TDM}}^{\text{up}}$ and another BPF window for a wavelength channel within Λ_{OLT} or Λ_{AWG} . More precisely, for a WDM ONU the first transmission grant specifies the allocated TDM transmission window on $\lambda_{\text{TDM}}^{\text{up}}$ used by the WDM ONU to send data,

if any, and the next REPORT message to the OLT. The second transmission grant specifies (i) the “best” wavelength channel within Λ_{OLT} , and (ii) the start time and duration of the BPF window during which the WDM ONU has to tune its BPF to the “best” wavelength for reception of data coming from the OLT and transmission of data going to the OLT. Note that the two windows assigned to a given WDM ONU are allowed to overlap in time (partly or fully in any arbitrary way). LR ONUs are handled the same way as WDM ONUs, except that the OLT can assign an additional BPF window on Λ_{AWG} to a given source LR ONU for transmission of eligible traffic if the destination ONU is an LR ONU (which is known by the OLT through the piggybacked destination ONU address in the respective REPORT message). In case of a destination LR ONU, the second transmission grant in the GATE message specifies (i) the appropriate wavelength channel within Λ_{AWG} that interconnects the source LR ONU with the destination LR ONU across the AWG and (ii) the start time and duration of the BPF window during which the source LR ONU has to tune its BPF to the selected wavelength for reception of data coming from the OLT and transmission of data going to the destination LR ONU, thereby optically bypassing the OLT. Otherwise, if the destination ONU is not an LR ONU, the source LR ONU is handled similar to a WDM ONU, as discussed above.

D. Dynamic Bandwidth Allocation

The OLT dynamically allocates bandwidth on Λ_{OLT} and Λ_{AWG} to its attached ONUs using the *gated* service discipline, i.e., the OLT does not impose any limit on the granted transmission windows and assigns each ONU as much bandwidth as requested in its REPORT message.

E. Access Control on Ring and PSC

RPR ring nodes as well as ONUs unable to send and receive data across the AWG, send their data on the tree, ring, and/or PSC (typically along the shortest path in terms of hops). Channel access on the dual-fiber ring is governed by RPR protocols, described in Section IV-E. On the PSC, time is divided into periodically recurring frames. Each frame on control channel λ_c consists of P control slots, each dedicated to a different CO. Each CO stores data packets to be forwarded on the PSC. For each stored data packet the CO broadcasts a control packet on the PSC to all COs in its assigned control slot. A control packet consists of two fields: (i) destination address and (ii) length of the corresponding data packet. After τ_{star} , all COs receive the control packet and build a common distributed transmission schedule for collision-free transmission of the corresponding data packet on the home channel(s) of the destination CO at the earliest possible time. The destination CO forwards the received data packet toward the final destination node.

VI. CAPACITY ANALYSIS

A. Network Model

Let C_T^k , C_W^k , C_A , C_P , and C_{RPR} denote the transmission capacities [in bits per second] of one TDM, WDM, AWG, PSC, and RPR channel, respectively, whereby k indexes the central office (CO) that the TDM or WDM channel connects to. We assume that both TDM upstream and downstream channel at CO k have each a capacity of C_T^k . We denote W^k for the number of WDM channels connecting to CO k , whereby each channel has capacity C_W^k . We define these capacities as ‘‘payload’’ transmission capacities in the sense that they already account for overheads that are proportional to the transmitted payload, such as the Preamble and Inter Packet Gap. The fixed overheads per grant, such as MPCP Report and guard times, are not considered.

We denote \mathcal{N} for the set of nodes that act as (payload) traffic sources and destinations. Specifically, \mathcal{N} contains all ONUs in the tree subnetworks, the RPR ring nodes, and the hotspot nodes (whereby there may be none, one, or several hotspots). The COs, except for the hotspots, do not locally generate traffic. We denote \mathcal{C}_k for the set of all ONUs that are connected to CO k . Additionally, we denote \mathcal{C}_k^T for the set of TDM ONUs connected to CO k , and analogously \mathcal{C}_k^W for the set of WDM ONUs connected to CO k , and \mathcal{C}_k^L for the set of LR ONUs attached to ONU k .

We model the packet generation rates by a traffic matrix $T = (T(i, j))$, $i, j \in \mathcal{N}$, where $T(i, j)$ represents the number of packets per second that are generated at a node i and are destined to node j . Note that for a network with $(P - H) \cdot N$ ONUs, N_r ring nodes, and H hotspot COs the traffic matrix has $((P - H) \cdot N + N_r + H) \times ((P - H) \cdot N + N_r + H)$ elements. For the stability analysis we assume that the traffic generation is ergodic and stationary. Importantly, the traffic matrix $T = (T(i, j))$, $i, j \in \mathcal{N}$, accounts only for the traffic that is *not* sent over the AWG. Since the operation of the AWG can be analyzed separately from the rest of the network, we consider AWG traffic separately in Section VI-A2. A natural assumption could be to assume that traffic is equally distributed from all ONUs to all other ONUs and/or RPR ring nodes, except possibly the hotspot(s). But we do not need to restrict our analysis to this special uniform traffic case.

We suppose that there is a packet length distribution (in bits) with mean \bar{L} and variance σ_L^2 . For notational simplicity we suppose that this distribution is the same for all source nodes. Note that, on average, node i sends $\bar{L} \cdot T(i, j)$ bits per second to node j .

1) *Traffic Rates in Ring/PSC Star Subnetwork:* First let us consider the traffic that is eventually sent over the ring/PSC star subnetwork. The traffic that arrives from the ONUs at CO k (over the conventional TDM or WDM channels) and is destined to another CO l , $l \neq k$, enters the ring/PSC star subnetwork. Hence, the packet rate of the ring/PSC star traffic between the two COs k and l , $k \neq l$, is given by

$$\sigma(k, l) := \sum_{i \in \mathcal{C}_k, j \in \mathcal{C}_l} T(i, j). \quad (1)$$

Note that traffic from an ONU i to another ONU j , $j \neq i$, attached to the same CO k , i.e., with $i, j \in \mathcal{C}_k$, does not enter the ring/PSC star subnetwork.

For an RPR ring node or a hotspot k and a CO l we define

$$\sigma(k, l) := \sum_{j \in \mathcal{C}_l} T(k, j), \quad (2)$$

and for a CO k and an RPR ring node or a hotspot l

$$\sigma(k, l) := \sum_{i \in \mathcal{C}_k} T(i, l). \quad (3)$$

Finally, for traffic from an RPR ring node/hotspot k to another RPR ring node/hotspot l , we have

$$\sigma(k, l) := T(k, l). \quad (4)$$

Note that the defined $\sigma(k, l)$ [in packets/second] completely determine the packet traffic rates in the ring/PSC star subnetwork.

For each node i , $i \in \mathcal{N}$, we denote

$$\sigma(i) := \sum_{l \in \mathcal{N}} T(i, l), \quad (5)$$

for the total packet traffic generation rate (in packets/second) at node i . Note that this packet rate only accounts for the traffic that is *not* sent over the AWG.

2) *Traffic Rates in AWG Star Subnetwork*: In addition to traffic that is sent over the tree and ring/PSC star subnetwork, an LR ONU or hotspot may generate traffic that is eligible for transmission over the AWG via the p2p/p2mp links. We suppose that an LR ONU/hotspot that generates a packet for another LR ONU/hotspot that *can* be reached via the AWG, i.e., there exists a p2p/p2mp link between the considered LR ONUs/hotspots, *will* send that packet over the AWG, and *not* over tree and ring/PSC star subnetworks. Formally, we let $c(k, l)$ denote the number of wavelength channels on the p2p/p2mp link between CO k and CO l . We denote $T^A(i, j)$ for the packet traffic rate in number of generated packets per second from LR ONU/hotspot i to LR ONU/hotspot j . If $c(k, l) = 0$, i.e., if there is no p2p/p2mp link from LR ONU $i \in \mathcal{C}_k^L$ to LR ONU $j \in \mathcal{C}_l^L$, then $T^A(i, j) = 0$. For LR ONU/hotspot i , we define

$$\sigma^A(i) := \sum_{l \in \mathcal{N}} T^A(i, l), \quad (6)$$

as the total packet generation rate [in packets/second] of traffic transmitted over the AWG. Note that an LR ONU/hotspot i may also generate traffic that is transmitted over the tree and ring/PSC star subnetwork; specifically, for RPR ring node, TDM ONU, and WDM ONU destinations, or for LR ONU/hotspot destinations not reachable from LR ONU/hotspot i via the AWG. This “non-AWG” traffic is accounted for in $\sigma(i)$ given by (5).

B. Capacity of EPON Tree Subnetwork

1) *Upstream Capacity*: Each ONU must not generate more traffic than it can send in the long term average. A TDM ONU can only transmit on the upstream TDM channel, whereas a WDM or LR ONU can transmit on the upstream TDM channel and one WDM channel.

$$\bar{L} \cdot \sigma(i) < \begin{cases} C_T^k & i \in \mathcal{C}_k^T \\ C_W^k + C_T^k & i \in \mathcal{C}_k^W \cup \mathcal{C}_k^L \end{cases} \quad (7)$$

Similarly, we require for each LR ONU that

$$\bar{L} \cdot \sigma^A(i) < C_A. \quad (8)$$

All TDM ONUs at a given CO k considered together must not transmit more than C_T^k on the upstream TDM channel

$$\lambda^{T,u,k} := \sum_{i \in \mathcal{C}_k^T} \bar{L} \cdot \sigma(i) < C_T^k. \quad (9)$$

The WDM and LR ONUs can send over the WDM channels and they can use the remaining bandwidth of the upstream TDM channel:

$$\lambda^{W,u,k} := \sum_{i \in \mathcal{C}_k^W \cup \mathcal{C}_k^L} \bar{L} \cdot \sigma(i) < W^k C_W^k + C_T^k - \lambda^{T,u,k}. \quad (10)$$

We note that the RSOA operation does not reduce the capacity. The finite (bounded) switchover time from one transmission direction to the other becomes negligible when queues grow long. In particular, for heavy traffic load and correspondingly very long continuous upstream or downstream transmissions, the switchover time becomes negligible. However, the RSOA operation has an impact on the delay, as analyzed in Section VII-B.

2) *Downstream Capacity*: The traffic arriving for the TDM ONUs has to be accommodated on the downstream TDM channel:

$$\lambda^{T,d,k} := \sum_{j \in \mathcal{C}_k^T} \sum_{l \in \mathcal{N}} \bar{L} \cdot T(l, j) < C_T^k. \quad (11)$$

The WDM channels may be used for upstream or downstream transmission. We investigate two possibilities.

a) *Reflection of Downstream Data Signal for Upstream Data Transmission*: Suppose the ONUs are equipped with a device that allows to use the downstream data signal as carrier signal for upstream data transmission. The OLT would either send downstream data; or, if there is no data to be sent, it would transmit ‘empty’ carrier. For this operating scenario, upstream and downstream transmissions are completely independent.

The restriction for upstream traffic is given in (10). For the downstream traffic we obtain

$$\lambda^{W,d,k} := \sum_{j \in \mathcal{C}_k^W \cup \mathcal{C}_k^L} \sum_{l \in \mathcal{N}} \bar{L} \cdot T(l, j) < W^k C_W^k + C_T^k - \lambda^{T,d,k}. \quad (12)$$

b) *Empty Carrier for Upstream Data Transmission*: If upstream data transmissions require an empty carrier signal, we can only use a WDM channel for either upstream or downstream transmission, resulting in the additional restriction that

$$\lambda^{W,d,k} + \lambda^{T,d,k} + \lambda^{T,u,k} + \lambda^{W,u,k} < C_T^k + W^k C_W^k. \quad (13)$$

C. Capacity of the Ring/PSC Star Subnetwork

Note that the $\sigma(k, l)$ defined above correspond to the respective $\sigma(i, j)$ in [47]. Further, we can introduce and calculate the analogous probabilities to $p_{k,l}(e)$ and $p_{k,l}(m, n)$ in [47]. Specifically, for our context, we introduce the probabilities $p_{i,j}(k, l)$ that traffic from a node $i \in \mathcal{N}$ to a node $j \in \mathcal{N}$ traverses the network link (k, l) . These probabilities can be precomputed for given traffic matrices T and T^A , similar to [47], for any pair of nodes in the network. The stability condition of the ring subnet is given by (8) in [47].

The mode of operation of the PSC in STARGATE is simpler than in [47], in that there are no collisions. Note that all traffic that is generated for destination CO l has to queue up in a *virtual queue* that is calculated by all COs. Therefore, for the capacity evaluations it suffices to require that $\lambda^P(l)$, the total rate of traffic (in bit/second) going from the PSC into CO l , does not overload the PSC wavelength channel

$$\lambda^P(l) := \sum_{\text{CO } k, k \neq l} \sum_{i,j \in \mathcal{N}} p_{i,j}(k, l) \cdot \bar{L} \cdot \sigma(i, j) < h(l)C_P, \quad (14)$$

whereby $h(l)$ denotes the number of home channels of CO l .

D. Capacity of the AWG

As noted in Section IV-F, the potential for collisions exists in the AWG star subnetwork only at the AWG input ports (local scheduling by the CO avoids actual collisions). For the capacity analysis, it suffices therefore to focus on the wavelength channels running from the LR ONUs at a given CO to the corresponding AWG input port. More specifically, the traffic generated by the LR ONUs of CO k destined toward LR ONUs at CO l must be accommodated on the wavelength channel(s) that are routed from the AWG input port of CO k to the AWG output port leading to CO l . Therefore, for analytical purposes, we can treat the AWG operation as if there were $c(k, l)$, $c(k, l) \geq 0$, separate wavelength channels from CO k to CO l , $l \neq k$. These channels do not influence each other (in terms of multiple access). Therefore, we obtain the following restriction for $\lambda^A(k, l)$, the total average rate of traffic (in bits/second) transmitted from CO (or hotspot) k over the AWG to CO (or hotspot) l :

$$\lambda^A(k, l) := \sum_{i \in \mathcal{C}_k^L, j \in \mathcal{C}_l^L} \bar{L} \cdot T^A(i, j) < C_A \cdot c(k, l). \quad (15)$$

If $c(k, l) = 0$, i.e., there are no wavelength channels from CO k to CO l over the AWG, the restriction has to be understood as $= 0$, not < 0 .

E. Summary of Capacity Analysis

We summarize the capacity analysis by noting that for given traffic patterns $T(i, l)$ and $T^A(i, l)$ it is relatively straightforward to obtain from the capacity constraints in Sections VI-B–VI-D bounds on the mean aggregate network throughput. In particular, we denote

$$r_T = \bar{L} \sum_{i \in \mathcal{N}} [\sigma(i) + \sigma^A(i)] \quad (16)$$

as the total generated traffic [in bit/second], which is equivalent to the total mean aggregate throughput of the network. Each capacity constraint results in an upper bound on r_T . The tightest bound identifies the network bottleneck limiting the mean aggregate throughput, as illustrated in Section VIII-B.

VII. DELAY ANALYSIS

For the delay analysis we consider a networking scenario with many legacy TDM ONUs and a few upgraded WDM and LR ONUs in the EPON subnetworks. For such a scenario, the traffic rate on the upstream TDM channel is typically significantly higher than on the WDM channels:

$$\sum_{i \in \mathcal{C}_k^W \cup \mathcal{C}_k^L} \sigma(i) \ll W^k \sum_{i \in \mathcal{C}_k^T} \sigma(i). \quad (17)$$

We leave the complementary scenario in which the WDM channels carry more load than the TDM channel for future work. In such a scenario the TDM channel becomes essentially a WDM channel since it will also be used by WDM and LR ONUs, leading to a situation where one can essentially neglect the special position of the TDM channel and consider it a WDM channel.

For the considered highly loaded TDM channel scenario, we have for the downstream TDM channel:

$$\lambda^{W,d,k} \ll W^k \lambda^{T,d,k}. \quad (18)$$

In the considered scenario with highly loaded TDM channels, the WDM and LR ONUs practically do not transmit or receive payload data on the TDM channels. This is in some sense an additional restriction, leading to a possibly higher delay, i.e., our analysis should lead to an upper bound for the delay. Note also that in the considered scenario the delays for reporting on the upstream TDM channel and transmitting grants on the downstream TDM channel are governed by the delays on the TDM channels.

We denote τ_T , τ_P , and τ_A [in seconds] for the one-way propagation delay over the EPON tree network, the PSC star subnetwork, and the AWG star subnetwork, respectively. For the delay analysis we require that the traffic that is generated at node i and destined to node j is Poisson with packet generation rate $T(i, j)$ [packets/second] and independent of the traffic for all other combinations i' , j' . For notational convenience, we define

$$\Phi(\rho) := \frac{\rho \left(\frac{\sigma_i^2}{\bar{L}} + \bar{L} \right)}{2C(1 - \rho)} \quad (19)$$

to denote the mean queuing delay in an M/G/1 queue according to the Pollaczek-Khinchine formula [48] as a function of the (relative) load ρ defined as the traffic rate λ [bit/second] normalized by the channel bit rate C [bit/second] for the considered packet size mean \bar{L} and variance σ_L^2 .

A. Delay on the Upstream and Downstream TDM channels

The long run average traffic rate on the downstream TDM channel from CO k is $\lambda^{T,d,k}$ given in (11), resulting in a load $\rho^{T,d,k} = \lambda^{T,d,k} / C_T^k$. Thus, an initial estimate of the queuing delay of a packet prior to transmission on the downstream TDM channel is approximately given by $\Phi(\rho^{T,d,k})$. This delay does not consider that this traffic has already traversed preceding nodes feeding into the downstream traffic at CO k . Specifically, the adjacent RPR nodes (via the RPR ring) and the other COs l , $l \neq k$ (via the PSC) supply downstream TDM traffic to CO k .

Applying the approximate method of Bux and Schlatter [49] to our setting, we compensate for the queuing delay at the preceding nodes by subtracting a correction term $B^{T,d,k}$ from the queuing delay $\Phi(\rho^{T,d,k})$ for the aggregate downstream traffic $\rho^{T,d,k}$. Following [49], the correction term $B^{T,d,k}$ is the sum of the queuing delays for the individual traffic stream that flow into CO k from adjacent nodes and leave over the arc of interest, namely the downstream TDM channel. In particular,

$$B^{T,d,k} = \sum_{\text{RPR node } l \text{ adjacent to CO } k} \Phi(\rho^{l,R,T,k}) + \sum_{\text{CO } l} \Phi(\rho^{l,P,T,k}). \quad (20)$$

with

$$\rho^{l,R,T,k} = \sum_{i \in \mathcal{N}} \sum_{j \in \mathcal{C}_k^T} p_{i,j}(l,k) T(i,j) \bar{L} / C_{RPR} \quad (21)$$

denoting the load due to traffic flowing from the adjacent RPR node l over the RPR ring to reach one of the TDM ONUs at CO k . For the evaluation of these traffic loads we utilize the probability $p_{i,j}(l,k)$ that traffic from a node $i \in \mathcal{N}$ to a node $j \in \mathcal{N}$ traverses the network link (l,k) , as defined in Section VI-C. Further, we evaluate

$$\rho^{l,P,T,k} = \sum_{i \in \mathcal{N}} \sum_{j \in \mathcal{C}_k^T} p_{i,j}(l,k) T(i,j) \bar{L} / C_P \quad (22)$$

for the load from a CO l , $l \neq k$, over the PSC to a TDM ONU at CO k .

Adding the average transmission delay \bar{L}/C_T^k and the downstream propagation delay τ_T we obtain the total delay as approximately

$$D^{T,d,k,E} := \Phi(\rho^{T,d,k}) + \tau_E + \frac{\bar{L}}{C_T^k} - B^{T,d,k}, \quad (23)$$

The mean of the residual cycle length on the upstream TDM channel until a generated packet is reported is approximately τ_T . In addition, there is a delay of $2\tau_T$ plus the residual transmission time of a packet when the downstream channel is busy, i.e., $\bar{L}/(2C_T) \cdot \rho^{T,d,k}$, between transmitting a report and receiving the corresponding grant. Adding queuing delay, packet transmission, and propagation delays gives

$$D^{T,u,k,E} = 4\tau_T + \Phi(\rho^{T,u,k}) + \frac{\bar{L}}{C_T} + \frac{\bar{L}}{2C_T} \rho^{T,d,k}. \quad (24)$$

Note that for our NG PON interconnection network there is an additional delay due to the queuing of the gate message prior to transmission on the downstream TDM channel. We consider two approaches for the downstream transmission of grant messages. (A) Without any priority for grant messages, the grant message has to queue up with regular downstream packet traffic, resulting in an additional delay component of $\Phi(\rho^{T,d,k})$. (B) A grant message could be given (non-preemptive) priority over data packets as follows. If there is currently no downstream data packet transmission ongoing, then immediately send the grant. If there is currently a downstream data packet transmission ongoing, then transmit the grant when the current packet transmission is complete. For this priority policy, the additional delay component is zero when the channel is idle and the residual transmission time of the packet when the channel is busy, i.e., $0 \cdot (1 - \rho^{T,d,k}) + \bar{L}/(2C_T^k) \cdot \rho^{T,d,k}$.

We remark that the analysis of the upstream TDM cycle length leading to (24) assumes a delay of $2\tau_T$ between sending the report and receipt of the corresponding grant. The grant has the additional delay component (of $\Phi(\rho^{T,d,k})$ or $\rho^{T,d,k}\bar{L}/2$) due to queuing of the grant prior to being transmitted on the downstream channel. Hence, the upstream TDM cycle is longer than reflected in our approximate analysis. A more exact analysis of the upstream TDM cycle that captures the inter-dependencies with the grant transmissions on the TDM downstream channel is left for future work.

B. Delay on the EPON WDM Channels

1) *Reflection of Downstream Data Signal for Upstream Data Transmission:* When reflecting the downstream data signal for upstream data transmission, the W^k WDM channels at CO k can be continuously used for downstream and upstream transmission. The traffic rate for the downstream WDM channels is given by $\lambda^{W,d,k}$ (12) and there are W^k channels, each with transmission rate C_W^k . The queuing delay could be approximated by the queuing delay in an M/G/ W^k queuing system. Since there is no explicit delay formula for such a system, we further approximate the delay by considering an M/G/1 queue with a server with transmission rate $W^k C_W^k$, i.e., we consider an M/G/1 queue with load $\rho^{W,d,k} = \lambda^{W,d,k}/(W^k C_W^k)$. We obtain the total delay as approximately,

$$D^{W,d,k,E} \approx \Phi\left(\frac{\lambda^{W,d,k}}{W^k C_W^k}\right) + \tau_T + \frac{\bar{L}}{C_T^k} - B^{W,d,k}, \quad (25)$$

where $B^{W,d,k}$ is defined analogously to (20), (21), and (22) with C_T^k replaced by $C_W^k \cup C_L^k$.

The upstream data transmissions have additional delay components due to the reporting and granting procedure:

- The residual time of the upstream TDM channel τ_T to account for the delay from packet generation until transmission of the corresponding report.
- the round trip propagation delay $2\tau_T$ to account for the upstream propagation of the report and downstream propagation of the grant.

- the queueing delay for the grant prior to its transmission on the downstream TDM channel, which is $\Phi(\rho^{T,d,k})$ without priority for grants, and $\rho^{T,d,k}\bar{L}/(2C)$ with priority for the grant messages (considered in (26)).

Thus, we obtain with the upstream traffic rate $\lambda^{W,u,k}$ defined in (10)

$$D^{W,u,k,E} \approx \tau_T + 2\tau_T + \frac{\rho^{T,d,k}\bar{L}}{2C_T^k} + \Phi\left(\frac{\lambda^{W,u,k}}{W^k C_W^k}\right) + \tau_T + \frac{\bar{L}}{C_W}. \quad (26)$$

2) *Empty Carrier for Upstream Data Transmission:* With switching between upstream and downstream transmission, the combined upstream and downstream traffic has to be accommodated on the C_k^W WDM channels, resulting in the load

$$\rho^{W,k} = \frac{\lambda^{W,d,k} + \lambda^{W,u,k}}{W^k C_W^k}. \quad (27)$$

which is served out of a (virtual) queue holding both upstream and downstream traffic. The resulting queueing delay is approximately $\Phi(\rho^{W,k})$.

If an empty carrier is used for upstream data transmissions, a waiting period equal to the one-way propagation delay τ_T is introduced when switching a WDM channel from upstream to downstream transmission, or vice versa. More specifically, when switching from downstream to upstream transmission, once the downstream transmission has ended, the immediately subsequently transmitted carrier signal takes τ_T to reach the ONU. Once the carrier signal starts to arrive at the ONU, it can immediately commence its upstream data transmission. Similarly, when switching from upstream to downstream transmission, the last bit of the upstream data transmission requires τ_T to reach the OLT. Only when the last bit of the upstream transmission has reached the OLT, can the OLT commence a new downstream data transmission.

We denote by $p_{s,k}$ the probability that a ‘switchover’ between upstream and downstream transmission, or vice versa, takes place before a data transmission on the WDM channels at CO k . Consider the superposition of two independent sequences of Poisson arrival times with rates λ_1 and λ_2 , respectively. Let P_1 be the event of an arrival from the first process (resp. denote P_2 for an arrival of the second process) and let SO denote the event that a switchover occurs. Then, the probability for a switchover equals

$$\mathbb{P}(SO) = \mathbb{P}(SO|P_1)\mathbb{P}(P_1) + \mathbb{P}(SO|P_2)\mathbb{P}(P_2) = \frac{\lambda_2}{\lambda_1 + \lambda_2} \cdot \frac{\lambda_1}{\lambda_1 + \lambda_2} + \frac{\lambda_1}{\lambda_1 + \lambda_2} \cdot \frac{\lambda_2}{\lambda_1 + \lambda_2}. \quad (28)$$

Note that the probability that a switchover occurs, given that we consider an arrival of the first process, is equal to the probability that an exponential random variable with mean $1/\lambda_2$ is smaller than another (independent) exponential random variable with mean $1/\lambda_1$. Simplifying, we obtain

$$p_{s,k} = \frac{2\lambda_1\lambda_2}{(\lambda_1 + \lambda_2)^2}, \quad (29)$$

whereby, noting that we consider CO k , we have the downstream traffic rate $\lambda^{W,d,k}$ and the upstream traffic rate $\lambda^{W,u,k}$ sharing the W^k channels, each with capacity C_W^k , i.e., $\lambda_1 := \lambda^{W,d,k}/(W^k C_W^k)$ and $\lambda_2 := \lambda^{W,u,k}/(W^k C_W^k)$.

For each switchover we calculate a loss of transmission time of τ_T . We model the switchovers as changes in the packet length distribution: the packet transmission time is extended by $C_W^k \tau_T$ with probability $p_{s,k}$. This gives a new mean of the packet distribution of $\bar{L} + p_{s,k} C_W^k \tau_T$ and second moment $\sigma_L^2 + 2\bar{L} p_{s,k} C_W^k \tau_T + p_{s,k} (C_W^k \tau_T)^2$. Using this modified message length distribution, we obtain the delay on the WDM channels as

$$D^{W,d,k} = \Phi(\rho^{W,k}) + \tau_T + \frac{\bar{L}}{C_T^k} - B^{W,d,k}. \quad (30)$$

The upstream traffic experiences additional delay components:

- The residual time of the upstream TDM channel τ_T to account for the delay from packet generation until transmission of the corresponding report.
- the round trip propagation delay $2\tau_T$ to account for the upstream propagation of the report and downstream propagation of the grant.
- the queueing delay for the grant prior to its transmission on the downstream TDM channel, which is $\Phi(\rho^{T,d,k})$ without priority for grants, and $\rho^{T,d,k} \bar{L}/2$ with priority for the grant messages (considered in (31)).

$$D^{W,u,k} := \tau_T + \frac{\rho^{T,d,k} \bar{L}}{2C_T^k} + 2\tau_T + D^{W,d,k}. \quad (31)$$

C. Delay on GPON

Let δ denote the frame duration of 125 μ s of the GPON. Consider a packet being generated at an ONU attached to OLT k . The packet has to wait on average $\delta/2$ for the beginning of the next frame in which it will be included in a dynamic bandwidth report (DBRu) field. This next frame has a duration (transmission delay) of δ and takes τ_T to propagate to the OLT.

Once arrived at the OLT, the bandwidth report has to be processed by the OLT and the grant to the ONU for the packet's transmission is included in the bandwidth map (BWmap) of the next downstream frame. Even with negligible processing time at the OLT, there is a delay of up to δ until the beginning of the next downstream frame. More specifically, let ω , $0 \leq \omega < \delta$, [in seconds] denote the offset between the up and down channels defined as follows. At the instant when a new slot starts on the upstream channel, ω seconds have passed of the current downstream channel slot, i.e., for $\omega = 0$, the slots on the upstream and downstream channels are aligned. Then, the time until the beginning of the downstream frame containing the BWmap of the considered packet is

$$\gamma_1 = \left(\left\lfloor \frac{\tau_T - \omega}{\delta} \right\rfloor + 1 \right) \delta - (\tau_T - \omega) \quad (32)$$

$$= \left(1 - \left(\frac{\tau - \omega}{\delta} - \left\lfloor \frac{\tau - \omega}{\delta} \right\rfloor \right) \right) \delta. \quad (33)$$

The downstream frame has a transmission delay of δ and propagation delay of τ_T . The packet has to wait for

$$\gamma_2 = \left(\left\lfloor \frac{\tau_T + \omega}{\delta} \right\rfloor + 1 \right) \delta - (\tau_T + \omega) \quad (34)$$

$$= \left(1 - \left(\frac{\tau + \omega}{\delta} - \left\lfloor \frac{\tau + \omega}{\delta} \right\rfloor \right) \right) \delta \quad (35)$$

until the beginning of the next upstream frame before it can possibly be transmitted. Thus, it takes overall on average $\delta/2 + \tau_T + \gamma_1 + \tau_T + \gamma_2$ from the instant the packet is generated to the instant the packet becomes eligible for upstream transmission. And then, the packet is put into a general queue for the upstream channel. In terms of the mean packet delay, this channel can be modeled as an M/G/1 queue (noting that the specific scheduling discipline does not affect the overall mean packet delay in the GPON, as long as the channel is operated in work conserving manner, i.e., is not left idle while packets are queued), with corresponding delay $\Phi(\rho^{T,u,k})$. Finally, the packet experiences the transmission delay \bar{L}/C_T^k and propagation delay τ_T . Overall, the mean delay for the TDM upstream channel is

$$D^{T,u,k,G} = \frac{5\delta}{2} + \gamma_1 + \gamma_2 + \Phi(\rho^{T,u,k}) + 3\tau_T + \frac{\bar{L}}{C_T^k}. \quad (36)$$

Analogously, we obtain for the WDM upstream channels which experience the same delays for the report-grant cycle but carry the load $\lambda^{W,u,k}/(W^k C_W^k)$:

$$D^{W,u,k,G} = \frac{5\delta}{2} + \gamma_1 + \gamma_2 + \Phi\left(\frac{\lambda^{W,u,k}}{W^k C_W^k}\right) + 3\tau_T + \frac{\bar{L}}{C_T^k}. \quad (37)$$

Note that ω can be adjusted to save up to one δ of delay. Specifically, there are two cases in the minimization of $\gamma_1 + \gamma_2$:

(A) If

$$\tau/\delta - \lfloor \tau/\delta \rfloor < \lfloor \tau/\delta \rfloor + 1 - \tau/\delta, \quad (38)$$

then any ω with

$$\tau/\delta - \lfloor \tau/\delta \rfloor < \omega/\delta < \lfloor \tau/\delta \rfloor + 1 - \tau/\delta \quad (39)$$

is optimal.

(B) If

$$\tau/\delta - \lfloor \tau/\delta \rfloor > \lfloor \tau/\delta \rfloor + 1 - \tau/\delta, \quad (40)$$

then any ω with

$$0 \leq \omega/\delta < \lfloor \tau/\delta \rfloor + 1 - \tau/\delta \quad (41)$$

is optimal.

Turning to the downstream transmission, we note that a packet arriving at the OLT has to wait on average $\delta/2$ for the beginning of the next downstream frame, i.e., before it becomes eligible for transmission. The

packet also experiences the average downstream queueing delay $\Phi(\rho^{T,d,k})$, transmission delay, propagation delay, and delay correction analogous to (23) for a total delay of approximately

$$D^{T,d,k,G} := \frac{\delta}{2} + \Phi(\rho^{T,d,k}) + \tau_T + \frac{\bar{L}}{C_T^k} - B^{T,d,k}, \quad (42)$$

The delay for the downstream WDM channels is obtained by replacing $\Phi(\rho^{T,d,k})$ by $\Phi\left(\frac{\lambda^{W,d,k}}{W^k C_W^k}\right)$ in (42).

D. Delay in the Ring/PSC Star Subnetwork

We first evaluate the packet delay in the PSC star subnetwork as follows. With τ_P^f denoting the frame duration [in seconds] on the PSC, a newly arrived packet at the CO waits on average $\tau_P^f/2$ before its control packet can be sent. The control packet experiences a propagation delay of τ_P . Once the control packet is received, the packet enters the virtual queue for the destination CO. This queue experiences a load of $\rho^{P,l} = \lambda^P(l)/C_P$ with $\lambda^P(l)$ given in (14). Adding in the transmission and propagation delays of the data packet over the PSC, we obtain

$$D^P(l) = \frac{1}{2}\tau_P^f + \tau_P + \Phi(\rho^{P,l}) + \tau_P + \frac{\bar{L}}{C_P} - B^{P,l}, \quad (43)$$

where $B^{P,l}$ is a correction term given by

$$B^{P,l} = \sum_{\text{CO } k} \left[\sum_{\text{RPR } m \text{ adjacent to CO } k} \Phi(\rho^{RPR,P,m,k,l}) + \Phi(\rho^{T,P,k,l}) + \Phi(\rho^{W,P,k,l}) \right] \quad (44)$$

with

$$\rho^{m,R,P,k,l} = \sum_{m,j \in \mathcal{N}} p_{mj}(m,k)p_{mj}(k,l)T(m,j)\bar{L}/C_{RPR} \quad (45)$$

denoting the traffic that originates at RPR node m and flows over the PSC from CO k to CO l . Analogously, we define

$$\rho^{T,P,k,l} = \sum_{i \in \mathcal{C}_T^k, j \in \mathcal{N}} p_{ij}(k,l)T(i,j)\bar{L}/C_T \quad (46)$$

and the respective quantity $\rho^{W,P,k,l}$, where \mathcal{C}_T^k is replaced by $\mathcal{C}_W^k \cup \mathcal{C}_L^k$ and C_T by C_W^k .

The packet delay in the ring D_{ij}^R from a CO/hotspot i to another CO/hotspot (or a destination ring node) j is given by Eqn. (22) in [47] with last two sums replaced by

$$D_{ij}^P = \sum_{k,l} p_{ij}(k,l)D^P(l). \quad (47)$$

Note that all links (k,l) that are not used for the transmission from node i to node j have $p_{ij}(k,l) = 0$ in the sum above. The packet delay from an RPR ring node to a CO/hotspot (or a destination RPR ring node) is given by Eqn. (21) in [47] with the last sum replaced by D_{ij}^P .

E. Delay in AWG Star Subnetwork

The packet delay in the AWG star subnetwork consists of the following components:

- The residual cycle time of the upstream TDM channel τ_T to account for the delay from packet generation until transmission of the corresponding report.
- The round trip propagation delay $2\tau_T$ to account for the upstream propagation of the report and downstream propagation of the grant.
- The queueing delay for the grant prior to its transmission on the downstream TDM channel, which is $\Phi(\rho^{T,d,k})$ without priority for grants, and $\rho^{T,d,k}\bar{L}/2$ with priority for the grant messages (considered in (48)).
- The queueing delay due to several LR ONUs with total load $\rho^A(k,l) = \lambda^A(k,l)/(c(k,l)C_A)$ sharing the $c(k,l)$ channels from CO k to CO l .
- The average packet transmission delay \bar{L}/C_A and propagation delay τ_A .

Thus, approximately,

$$D^A(k,l) = +3\tau_T + \frac{\rho^{T,d,k}\bar{L}}{2C_T^k} + \Phi(\rho^A(k,l)) + \tau_A + \frac{\bar{L}}{C_A}. \quad (48)$$

Note that the first two terms in the this expression only occur because the LR ONUs have to use the upstream TDM channel to register their packets. By averaging over all channels we obtain the average packet delay on the AWG star subnetwork:

$$D^A = \sum_{\text{CO } k,l} D^A(k,l) \cdot \frac{\lambda^A(k,l)}{\sum_{\text{CO } k',l'} \lambda^A(k',l')}. \quad (49)$$

F. The Hotspots

Note that the hotspot nodes do not require any special analysis. The hotspots simply have typically a higher traffic volume, which is expressed in the respective $T(i,j)$ and $T^A(i,j)$. A hotspot node is modeled as any other RPR ring node (or CO) in the ring/PSC star subnetwork, and as a CO in the AWG star subnetwork.

G. Overall Delay

We obtain the overall average packet delay by weighing the different paths according to their packet traffic rates. First, for traffic transmitted over the ring/PSC star subnetwork:

$$D^{R,P} = \sum_{i,j} D(i,j) \frac{T(i,j)}{\sum_{i',j'} T(i',j')}, \quad (50)$$

where

- $D(i,j) = D_{ij}^R$ for traffic from RPR ring node/hotspot i to RPR ring node/hotspot j .
- $D(i,j) = D_{il}^R + D^{T,d,l}$ for traffic from RPR ring node/hotspot i to TDM ONU j at CO l (resp. $D^{W,d,l}$ for traffic to WDM or LR ONU at CO l).

- $D(i, j) = D^{T,u,k} + D_{kl}^R + D^{T,d,l}$ for traffic from TDM ONU i at CO k to TDM ONU j at CO l (resp. $D^{W,u,k}$ for traffic from WDM or LR ONU i at CO k and resp. $D^{W,d,l}$ for traffic to WDM or LR ONU j at CO l). Note that for intra-CO traffic from an ONU i to another ONU j attached to the same CO k , $D(i, j)$ gives the intra-CO as $D^{T,u,k} + 0 + D^{T,d,k}$ (since the ring delay is zero for $k = l$); the scenarios with intra-CO traffic to and/or from a WDM ONU are captured analogously.
- $D(i, j) = D^{T,u,k} + D_{kj}^R$ for traffic from TDM ONU i at CO k to RPR ring node/hotspot j (resp. $D^{W,u,k}$ for traffic from WDM or LR ONU i at CO k).

Overall we obtain:

$$D = D^{R,P} \frac{\sum_{i,j} T(i, j)}{\sum_{i,j} T(i, j) + \sum_{\text{LR ONUs } i,j} T^A(i, j)} + D^A \frac{\sum_{\text{LR ONUs } i,j} T^A(i, j)}{\sum_{i,j} T(i, j) + \sum_{\text{LR ONUs } i,j} T^A(i, j)}. \quad (51)$$

VIII. NUMERICAL AND SIMULATION RESULTS

This section presents numerical results on the throughput-delay performance, first for isolated PONs and then for integrated access-metro networks, obtained from our analysis and extensive verifying simulations with 95% confidence intervals. The propagation speed is set to $2 \cdot 10^8$ m/s. We first consider uniform traffic where each ONU generates the same amount of packet traffic with a packet size randomly uniformly distributed over [64, 1518] bytes. In the context of an isolated PON, a packet generated by a given ONU is destined to any of the other $N - 1$ ONUs of the same PON with equal probability $1/(N - 1)$.

A. Isolated PONs

Fig. 6 compares the mean delay D on the upstream TDM/WDM channels of conventional TDM, high-speed TDM, and WDM EPON/GPON networks vs. the mean aggregate throughput r_T . We consider an EPON with $C_T = 1$ Gb/s and a (symmetric) GPON with $C_T = 1.25$ whereby the ONUs are located at 20 km from the OLT. We consider a fixed number of $N_T = 32$ TDM ONUs and $N_W = 32$ WDM ONUs, respectively. Both high-speed TDM PONs operate at a data rate of $C_T \in \{2.5, 10\}$ Gb/s. In addition to the pair of legacy TDM wavelength channels, the WDM EPON and WDM GPON deploy $W \in \{2, 8\}$ wavelength channels via remodulation, each operating at $C_W = C_T = 1$ Gb/s and $C_W = C_T = 1.25$ Gb/s, respectively. We observe that the EPON achieves significantly lower delays than the GPON at small to medium traffic loads. This EPON advantage is due to its underlying variable-length polling cycle compared to the fixed length framing structure of the GPON. We further observe that analysis and simulation results match very well, except that the analysis underestimates the mean EPON delay slightly at medium traffic loads.

Fig. 7 shows the 10 Gb/s high-speed TDM and WDM EPON/GPON with remodulation of Fig. 6 and compares them to a WDM EPON/GPON using the commercially available empty carrier approach [4]. The empty carrier approach severely deteriorates the performance of both WDM EPON and WDM GPON, suffering from a higher mean delay and a significantly lower mean aggregate throughput on the upstream

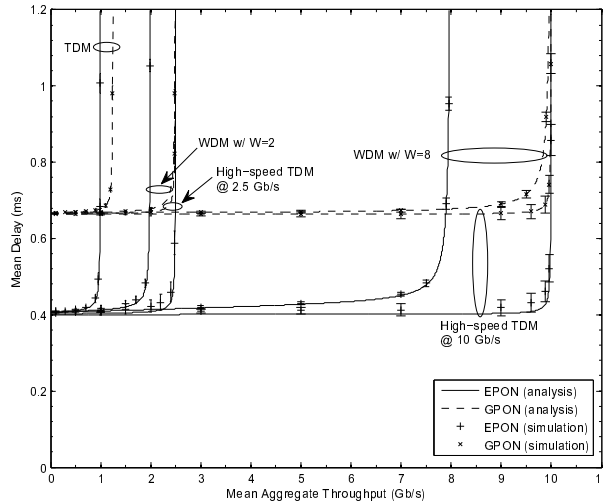


Fig. 6. Mean delay D on upstream TDM/WDM channels of high-speed TDM and WDM EPON/GPON vs. mean aggregate throughput r_T for $N_T = 32$ TDM ONUs and $N_W = 32$ WDM ONUs, respectively.

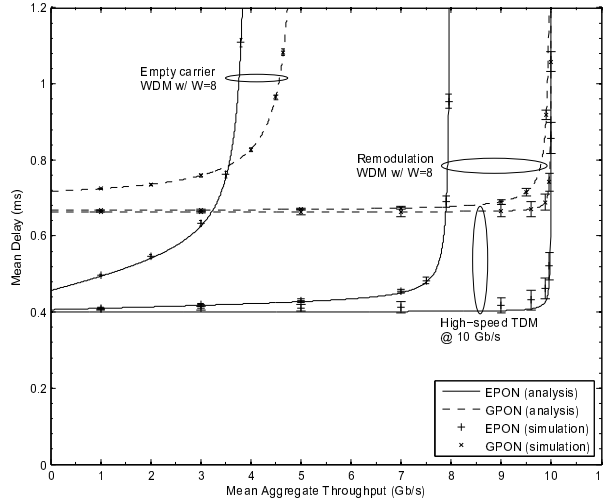


Fig. 7. Mean delay D vs. mean aggregate throughput r_T of WDM EPON/GPON using remodulation and empty carrier.

TDM/WDM channels than a WDM EPON/GPON based on remodulation. This is due to the fact that in the empty carrier approach each WDM wavelength channel is used for bidirectional transmission, i.e., upstream and downstream transmissions alternate, as opposed to remodulation where upstream transmissions are not delayed by downstream transmissions.

B. Integrated Access-Metro Networks

Next, we investigate different methods to interconnect multiple high-speed TDM/WDM PONs by means of a ring, PSC, and/or AWG. Fig. 8 depicts the mean delay vs. mean aggregate throughput of three of the aforementioned WDM EPONs/GPONs interconnected through either (i) a ring only, or (ii) a ring in conjunction with a 4×4 PSC (i.e., $P = 4$), for shortest path (minimum hop) routing. The circumference

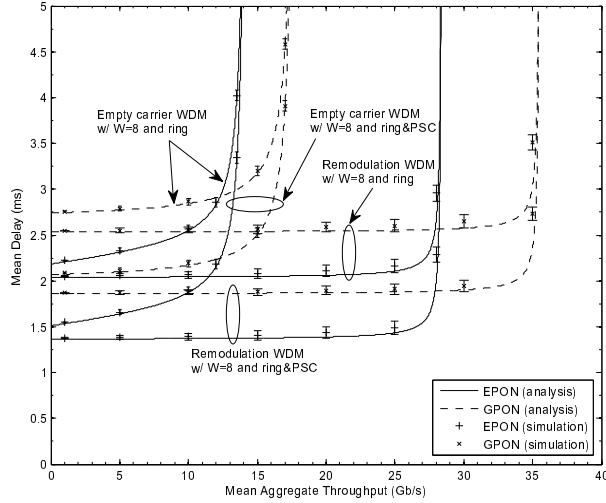


Fig. 8. Mean delay D vs. mean aggregate throughput r_T of three WDM PONs interconnected through (i) a ring, or (ii) a ring combined with a 4×4 PSC.

of the bidirectional ring is set to 100 km and it comprises $N_r = 4$ equally spaced ring nodes. Both ring and PSC operate at a data rate of 10 Gb/s, i.e., $C_R = C_P = 10$ Gb/s. We consider uniform source and destination traffic originating from and going to any of the $3 \cdot 32 = 96$ WDM ONUs, $N_r = 4$ ring nodes, and $H = 1$ remote CO (see Fig. 2). Formally, for uniform source traffic, $\sigma(i) = \sigma \forall i \in \mathcal{N}$ and the total traffic bit rate in the network is $r_T = \eta \bar{L} \sigma$. As shown in Fig. 8, using a PSC that provides short-cut links to the ring helps decrease the mean delay considerably, but in the considered example network configuration does not lead to an increased mean aggregate throughput. (Similar observations were made for 10 Gb/s high-speed TDM PONs, not shown here due to space constraints.) In particular, for the EPON with uniform source and uniform destination traffic, both the upstream (Eqn. (10)) and the downstream WDM channel with remodulation capacity constraint (Eqn. (12)) give the bound

$$r_T < \frac{\eta(\eta - 1)(W + 1)C}{(\eta - 1)(N_T + N_W) + \eta_{TW_r} N_L} \quad (52)$$

with $\eta_{TW_r} = (P - H)(N_T + N_W) + N_r$ denoting the total number of TDM/WDM ONUs and ring nodes. For the considered scenarios with $N_W = 32$ WDM ONUs (and no TDM or LR ONUs) this bound reduces to $r_T < \eta(W + 1)C/N_W = 28.4$ Gbps, which is lower than the bounds imposed by the ring and PSC, as detailed next, and hence governs the maximum mean aggregate throughput.

For further analysis of the ring/PSC stability condition (14), we fix the ring network to the structure illustrated in Fig. 2 with $N_r = 4$ ring nodes, $P = 4$ OLTs (of which $H = 1$ is a remote CO), and with one ring node between two OLTs. The highest traffic rate on a PSC channel arises for the uniform traffic pattern on the channel toward an OLT when the remote CO is two ring hops from the considered OLT. We refer henceforth to the considered OLT as the “target OLT”, the OLT opposite of the target OLT around the ring as the “opposite OLT”, and the OLT situated two hops along the ring from the target OLT as the

“adjacent OLT” (which is located opposite the remote CO). We have the following contributions to the traffic load on the PSC home channel of the target OLT:

- The opposite OLT has $N_T + N_W$ TDM/WDM ONUs sending (i) to the N nodes in the EPON attached to the target OLT, plus (ii) with probability one half to the two ring nodes situated one hop from the target OLT over the target home channel. In addition, the opposite OLT has N_L LR ONUs sending (i) to the $N_T + N_W$ TDM/WDM ONUs in the EPON attached to the target OLT, plus (ii) with probability one half to the two ring nodes situated one hop from the target OLT over the target channel. Thus, the opposite OLT contributes

$$\frac{r_T}{\eta}(N_T + N_W)\frac{N + \frac{1}{2}2}{\eta - 1} + \frac{r_T}{\eta}N_L\frac{N_T + N_W + \frac{1}{2}2}{\eta - 1}. \quad (53)$$

- The adjacent OLT has the same contribution as the opposite OLT, except that only the traffic to EPON nodes attached to the target OLT is sent over the PSC; the ring nodes situated one hop from the target OLT are reached with one hop over the ring (versus two hops over the PSC and then ring). Furthermore, the remote CO contributes as much as one LR ONU at the adjacent CO. Overall, the contribution from the adjacent OLT and the remote CO is thus

$$\frac{r_T}{\eta}(N_T + N_W)\frac{N}{\eta - 1} + \frac{r_T}{\eta}(N_L + 1)\frac{N_T + N_W}{\eta - 1}. \quad (54)$$

- The two ring nodes situated within one ring hop from the target OLT do not send traffic toward the target OLT over the PSC.
- The two ring nodes situated three hops in either ring direction from the target OLT send to all ONUs attached to the target OLT over the PSC (and directly over the ring to the ring nodes one hop from the target OLT) contributing

$$\frac{r_T}{\eta}2\frac{N}{\eta - 1}. \quad (55)$$

Combining these contributions results in the constraint

$$r_T < \frac{\eta(\eta - 1)C_P}{d_1} \quad (56)$$

$$d_1 = (N_T + N_W)(3N + 1) + N_L(3N_T + 3N_W + 1) + 2N + N_T + N_W. \quad (57)$$

For our scenario with $N_L = 0$, $N_T = 0$ and $N = N_W$ this simplifies to

$$r_T < \frac{\eta(\eta - 1)C_P}{3N_W(N_W + 4/3)} = 31.5625\text{Gbps}. \quad (58)$$

In the following, we study the impact of non-uniform traffic on the throughput-delay performance of NG-PONs. Let us first focus on *non-uniform source traffic*, where nodes generate different traffic rates. For now, we continue to consider uniform destination traffic. More specifically, N_m of the ONUs in each NG-PON as well as all N_r ring nodes generate traffic at a medium bit rate of $\sigma\bar{L}$. Furthermore, we

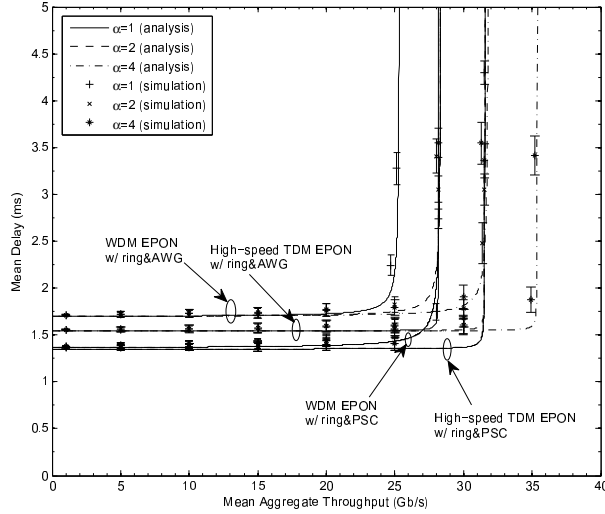


Fig. 9. Mean delay D vs. mean aggregate throughput r_T of three WDM EPONs and three high-speed TDM EPONs interconnected through (i) a ring&PSC, or (ii) a ring&AWG for different source traffic non-uniformity $\alpha \in \{1, 2, 4\}$.

introduce a source traffic non-uniformity α , $\alpha \geq 1$, and let N_l lightly loaded ONUs in each NG-PON generate traffic at a low bit rate of $\sigma \bar{L}/\alpha$, and N_h highly loaded ONUs in each NG-PON as well as the remote CO generate traffic at a high bit rate of $\alpha \sigma \bar{L}$. Note that $\alpha = 1$ denotes uniform traffic, which has been studied above.

Fig. 9 compares the mean delay vs. mean aggregate throughput performance of three WDM EPONs with $W = 8$ wavelengths in remodulation mode, each operating at 1 Gb/s, with that of three 10 Gb/s high-speed TDM EPONs, interconnected with the remote CO through a ring in conjunction with (i) a 4×4 PSC, or (ii) a 4×4 AWG using $\Lambda_{\text{AWG}} = 4$ wavelengths. The ring, PSC, and AWG operate at 10 Gb/s, i.e., $C_R = C_P = C_A = 10$ Gb/s. In each EPON, we set $N_l = 16$ and $N_m = N_h = 8$ and consider different source traffic non-uniformity $\alpha \in \{1, 2, 4\}$. In the ring&PSC configuration, there are $N_W = 32$ WDM ONUs in a given WDM EPON (resp. $N_T = 32$ ONUs in a high-speed TDM EPON). In the ring&AWG configuration, the N_h highly loaded ONUs are upgraded to LR-ONUs in each high-speed WDM EPON (and each high-speed TDM EPON which is connected with P high-speed wavelength channels to the AWG).

We observe from Fig. 9 that the ring&PSC configurations are insensitive to source traffic non-uniformities. This is because the shift in traffic generation from lightly to heavily loaded ONUs with increasing source traffic non-uniformity α does not significantly shift the portion of the total network traffic load that needs to traverse the EPON downstream WDM channels. In contrast, for the ring&AWG configurations we observe from Fig. 9 increases in the aggregate network throughput as the traffic becomes more non-uniform. With increasing α , the heavily loaded ONUs account for a larger portion of the total network traffic. Thus, the traffic portion that can be off-loaded from the EPON WDM channels to the AWG channels, namely

all traffic between pairs of heavily loaded ONUs, increases with α , resulting in an increased aggregate throughput. (Similar observations were made for high-speed TDM and WDM GPONs.)

The total traffic bit rate in the network is

$$r_T = \left[(P - H) \left(\frac{N_l}{\alpha} + N_m + \alpha N_h \right) + N_r + \alpha H \right] \sigma \bar{L}. \quad (59)$$

For notational convenience, we define the equivalent number of medium bit rate traffic nodes as

$$\eta_\alpha = (P - H) \left(\frac{N_l}{\alpha} + N_m + \alpha N_h \right) + N_r + \alpha H, \quad (60)$$

with which we express the medium traffic bit rate in terms of r_T as $\sigma \bar{L} = r_T / \eta_\alpha$. We focus first on the WDM EPON with ring&PSC scenario. Note that $\lambda^{T,u,k} = \lambda^{T,d,k} = 0$. For the upstream WDM channels we obtain by noting that all traffic generated at the nodes of a given EPON has to go up on the WDM (and TDM) channels

$$\lambda^{W,u,k} = \frac{r_T}{\eta_\alpha} \left(\frac{N_l}{\alpha} + N_m + \alpha N_h \right) \quad (61)$$

and the corresponding limit

$$r_T < \frac{\eta_\alpha (W + 1) C}{\frac{N_l}{\alpha} + N_m + \alpha N_h}. \quad (62)$$

For the considered scenario with $\eta = 101$, $\eta_1 = 101$, $\eta_2 = 102$, and $\eta_4 = 140$ we obtain the constraints $r_T < 28.40625$ for $\alpha = 1$, $r_T < 28.6875$ for $\alpha = 2$, and $r_T < 28.636364$ for $\alpha = 4$.

For the downstream WDM (and TDM) channels using remodulation we note that all traffic generated by one of the N nodes at the considered EPON and destined to any of the other $N - 1$ nodes at the EPON as well as any traffic generated by one of the other nodes in the network and destined to any of the N nodes at the EPON contributes to the downstream load

$$\begin{aligned} \lambda^{W,d,k} = \frac{r_T}{\eta_\alpha} & \left[\frac{N_l}{\alpha} \frac{N-1}{\eta-1} + N_m \frac{N-1}{\eta-1} + \alpha N_h \frac{N-1}{\eta-1} \right. \\ & + (P-H-1) \frac{N_l}{\alpha} \frac{N-1}{\eta-1} + (P-H-1) N_m \frac{N}{\eta-1} \\ & \left. + (P-H-1) \alpha N_h \frac{N}{\eta-1} + N_r \frac{N}{\eta-1} + \alpha H \frac{N}{\eta-1} \right], \end{aligned} \quad (63)$$

resulting in the limit

$$r_T < \frac{\eta_\alpha (\eta - 1) (W + 1) C}{d}. \quad (64)$$

with

$$\begin{aligned} d = (N - 1) & \left(\frac{N_l}{\alpha} + N_m + \alpha N_h \right) \\ & + N \left((P - H - 1) \left(\frac{N_l}{\alpha} + N_m + \alpha N_h \right) \right. \\ & \left. + N_r + \alpha H \right) \end{aligned} \quad (65)$$

For the considered scenario we obtain the limits $r_T < 28.40625$ for $\alpha = 1$, $r_T < 28.40346$ for $\alpha = 2$, and $r_T < 28.40397$ for $\alpha = 4$. Taken together, these capacity results confirm the simulation results for the ring&PSC configuration.

Next, we focus on the WDM EPON with ring&AWG. For the upstream WDM channels note that the N_l low traffic ONUs and the N_m medium traffic ONUs at a given EPON send all generated traffic upstream on the WDM (and TDM) channel. In addition the N_h high traffic ONUs send the traffic to nodes not connected to the AWG upstream on the WDM channels, i.e.,

$$\lambda^{W,u,k} = \frac{r_T}{\eta_\alpha} \left(\frac{N_l}{\alpha} + N_m + \alpha N_h \frac{\eta_{TW_r}}{\eta - 1} \right) \quad (66)$$

with

$$\eta_{TW_r} = (P - H)(N_l + N_m) + N_r \quad (67)$$

denoting the number of nodes not connected to the AWG. The corresponding capacity limit is

$$r_T < \frac{\eta_\alpha(W + 1)C}{\left(\frac{N_l}{\alpha} + N_m + \alpha N_h \frac{\eta_{TW_r}}{\eta - 1} \right)}. \quad (68)$$

We obtain for our scenario for which $\eta_{TW_r} = 76$, for $\alpha = 1$ $r_T < 30.2194$, for $\alpha = 2$ $r_T < 32.5994$, and for $\alpha = 4$ $r_T < 34.6916$.

For the AWG channels we obtain the highest load on the channels connecting two EPONs, namely

$$\lambda^A = \frac{r_T}{\eta_\alpha} \alpha N_h \frac{N_h}{\eta - 1} \quad (69)$$

and the corresponding limit

$$r_T < \frac{\eta_\alpha(\eta - 1)cC}{\alpha N_h^2}. \quad (70)$$

For our scenario, $r_T < 1578.125$ for $\alpha = 1$, $r_T < 796.875$ for $\alpha = 2$, and $r_T < 453.125$ for $\alpha = 4$.

Fig. 10 considers the ring&AWG configurations of the previous figure for a fixed source traffic non-uniformity $\alpha = 2$ and illustrates the impact of *non-uniform destination traffic*. Specifically, a packet generated by an LR ONU or CO is destined to another LR ONU/CO with probability $(\eta_{LH} - 1)/(\eta - 1) \leq \beta \leq 1$, whereby $\eta_{LH} = (P - 1)N_h + H$ denotes the number of LR-ONUs and CO in the network. Note that in our case $\beta = (\eta_{LH} - 1)/(\eta - 1) = 0.24$ corresponds to uniform destination traffic. We observe from Fig. 10 that both AWG network configurations are quite sensitive to destination traffic non-uniformity. The maximum mean aggregate throughput is significantly increased as the fraction of traffic routed over the AWG increases.

We illustrate the application of the capacity constraints of Sections VI-B–VI-D. The total traffic bit rate in the network is

$$r_T = \left[(P - H) \left(\frac{N_l}{\alpha} + N_m + \alpha N_h \right) + N_r + \alpha H \right] \sigma \bar{L}. \quad (71)$$

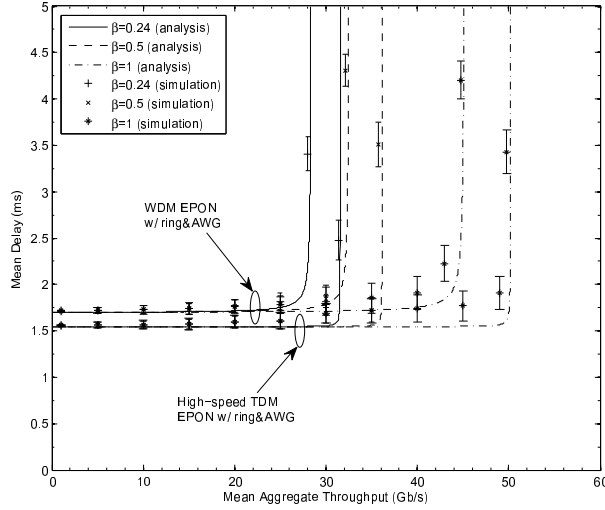


Fig. 10. Mean delay D vs. mean aggregate throughput r_T of three WDM EPONs and three high-speed TDM EPONs interconnected through a ring&AWG for $\alpha = 2$ and different destination traffic non-uniformity $\beta \in \{0.24, 0.5, 1\}$.

For notational convenience, we define the equivalent number of medium bit rate traffic nodes as

$$\eta_\alpha = (P - H) \left(\frac{N_l}{\alpha} + N_m + \alpha N_h \right) + N_r + \alpha H, \quad (72)$$

with which we express the medium traffic bit rate in terms of r_T as $\sigma \bar{L} = r_T / \eta_\alpha$.

For the upstream WDM channels, we note that an LR ONU sends a packet with probability $1 - \beta$ over the upstream WDM channels. Hence,

$$\lambda^{W,u} = \frac{r_T}{\eta_\alpha} \left[\frac{N_l}{\alpha} + N_m + \alpha N_h (1 - \beta) \right] \quad (73)$$

and

$$r_T < \frac{\eta_\alpha (W + 1) C_W}{\frac{N_l}{\alpha} + N_m + \alpha N_h (1 - \beta)}. \quad (74)$$

for our scenario for $\alpha = 2$ and $\eta_\alpha = 102$, we obtain for $\beta = 0.24$: $r_T < 32.59943 C_W$, for $\beta = 0.5$: $r_T < 38.25 C_W$, and for $\beta = 1$: $r_T < 57.375 C_W$.

For the WDM downstream channels when using signal reflection for upstream transmissions, traffic contributions are made by (i) the transmissions from the WDM ONUs at the considered EPON to the other WDM ONUs at the EPON, (ii) the transmissions by all other WDM ONUs and the ring nodes in the network to all the ONUs in the considered EPON, (iii) the transmissions by all the LR ONUs and the remote CO to the WDM ONUs in the considered EPON giving for (12):

$$\begin{aligned} \lambda^{W,d} = & \frac{r_T}{\eta_\alpha} \left[\left(\frac{N_l}{\alpha} + N_m \right) \frac{N_l + N_m - 1}{\eta - 1} \right. \\ & + \left. \left((P - H) \left(\frac{N_l}{\alpha} + N_m \right) + N_r \right) \frac{N}{\eta - 1} \right. \\ & \left. + \alpha \left((P - H) N_h + H \right) (1 - \beta) \frac{N_l + N_m}{\eta T W r} \right], \quad (75) \end{aligned}$$

Defining for the number of nodes not connected to the AWG $\eta_{TW_r} = (P - H)(N_l + N_m) + N_r$ and $\eta_{TWR\alpha} = (P - H)(\frac{N_l}{\alpha} + N_m) + N_r$ gives the limit

$$r_T < \frac{\eta_\alpha(W + 1)C_W}{\frac{(\frac{N_l}{\alpha} + N_m)(N_l + N_m - 1)}{\eta - 1} + \frac{\eta_{TWR\alpha}N}{\eta - 1} + \frac{\alpha(1 - \beta)\eta_{LH}(N_l + N_m)}{\eta_{TW_r}}}. \quad (76)$$

The resulting throughput limits are $r_T < 28.4$ Gbps for $\beta = 0.24$, $r_T < 32.5$ Gbps for $\beta = 0.5$, and $r_T < 45.2$ Gbps for $\beta = 1$.

For the AWG we obtain from (15) the highest load on the AWG channels interconnecting two EPONs as

$$\lambda^A = \frac{r_T}{\eta_\alpha} \alpha N_h \beta \frac{N_h}{\eta_{LH}} \quad (77)$$

and the corresponding limit

$$r_T < \frac{\eta_\alpha \eta_{LH} C_A}{\alpha \beta N_h^2}. \quad (78)$$

For our scenario, we obtain for $\beta = 1$ the aggregate throughput constraint $r_T < 199.2$ Gbps, indicating that the AWG channels are still utilized to less than 25%.

IX. CONCLUSIONS

We have developed a comprehensive probabilistic analysis for evaluating the packet throughput-delay performance of next-generation PONs (NG-PONs). Our analysis accommodates both EPONs and GPONs with their various next-generation upgrades, as well as a variety of all-optical interconnections of NG-PONs. Our numerical results illustrate the use of our analysis to evaluate the throughput delay performance of upgrades that increase the transmission line rates or wavelength counts. We also demonstrate the identification of network bottlenecks using our analysis.

APPENDIX

SPECIFIC CAPACITY LIMITS FOR UNIFORM AND NON-UNIFORM TRAFFIC

In this appendix we consider an NG-PON with three ring nodes between two OLTs/COs, whereas only one ring node is considered in Section VIII. Further, we consider in this appendix low traffic ONUs to be TDM ONUs, medium traffic ONUs to be WDM ONUs and high traffic ONUs to be LR ONUs; whereas, in Section VIII both low and medium traffic ONUs are considered WDM ONUs and high traffic ONUs are considered LR ONUs.

A. Uniform Source-Uniform Destination Traffic We initially consider uniform source traffic where all nodes generate the same traffic bit rate, i.e., $\bar{L}\sigma(i) = \bar{L}\sigma \forall i \in \mathcal{N}$, in conjunction with uniform destination traffic where a packet generated at a node i is destined to any of the other nodes with equal probability, i.e., $r(i, j) = r_i / (\eta - 1) \forall j \neq i$. Note that for the uniform source traffic,

$$r_T = \eta \bar{L}\sigma. \quad (79)$$

We consider EPON configurations with (a) $N_T = 32$, (b) $N_T = 24$, $N_W = N_L = 4$, (c) $N_T = 16$, $N_W = N_L = 8$, and (d) $N_T = 4$, $N_W = N_L = 14$. A given LR ONU/hotspot CO i sends all traffic destined to other LR ONUs/the hotspot CO j over the AWG subnetwork, i.e., $r^A(i) = [(P-2)N_L + N_L - 1 + 1]\sigma/(\eta-1)$, since there are N_L LR ONUs at each of the other COs, $N_L - 1$ other LR ONUs at the CO that the considered LR ONU i is attached to, and one hotspot. If transmission over the AWG is possible, the corresponding traffic rates $T(i, j)$ and $r(i, j)$ for traffic over the EPON and PSC/ring subnetwork are set to zero. That is, the total traffic generation rate at each node is constant, and the generated traffic is either sent over the EPON and PSC/ring subnetwork, or, if possible, over the AWG subnetwork.

From the stability conditions in Section VI, we readily see that for the TDM EPON channel the upstream condition (9) gives $\lambda^{T,u,k} = \frac{r_T}{\eta} N_T$ since each node generates a bit rate of $\frac{r_T}{\eta}$ and the N_T TDM nodes send all their traffic upstream on the TDM channel. Hence, the stability condition in terms of r_T takes the form

$$r_T < \frac{\eta C}{N_T}. \quad (80)$$

For the WDM EPON channel upstream condition (10), we note that the N_W WDM ONUs send all their upstream traffic and the N_L LR ONUs send all traffic not destined to other LR ONUs/hotspot, i.e., all traffic destined to TDM/WDM ONUs and ring nodes, upstream on the WDM channels (or the TDM channel). Denoting for notational convenience the number of TDM/WDM ONUs and ring nodes by

$$\eta_{TW_r} = (P - H)(N_T + N_W) + N_r, \quad (81)$$

we obtain $\lambda^{W,u,k} = \frac{r_T}{\eta} (N_W + N_L \frac{\eta_{TW_r}}{\eta-1})$, resulting in the condition

$$r_T < \frac{\eta(\eta-1)(W+1)C}{(\eta-1)(N_T + N_W) + \eta_{TW_r} N_L}. \quad (82)$$

For the downstream TDM channel, we note that the N_T TDM nodes at the considered EPON send a packet to one of the other $N_T - 1$ TDM nodes in the same EPON with probability $(N_T - 1)/(\eta - 1)$. The other $\eta - N_T$ nodes in the network send a packet to one of the N_T nodes in the considered EPON with probability $N_T/(\eta - 1)$. Thus,

$$\lambda^{T,d,k} = \frac{r_T}{\eta} \left[N_T \cdot \frac{N_T - 1}{\eta - 1} + (\eta - N_T) \frac{N_T}{\eta - 1} \right], \quad (83)$$

which simplifies to the stability condition (80).

For the downstream WDM channel condition for reflection of the downstream signal (12) there are three contributors to downstream WDM channel traffic: (i) the N_W WDM ONUs at the considered EPON sending to other WDM ONUs at this EPON contributing $\frac{r_T}{\eta} N_W \frac{N_W - 1}{\eta - 1}$, (ii) all other nodes in the network sending to the N_W WDM ONUs, contributing $\frac{r_T}{\eta} (\eta - N_W) \frac{N_W}{\eta - 1}$, and (iii) all TDM/WDM ONUs and ring nodes sending to the LR ONUs in the considered EPON contributing $\frac{r_T}{\eta} \eta_{TW_r} \frac{N_L}{\eta - 1}$, resulting in

$$\lambda^{W,d,k} = \frac{r_T}{\eta(\eta-1)} [(\eta-1)N_W + \eta_{TW_r} N_L]. \quad (84)$$

Inserting into (12) results in a condition identical to (82).

For upstream transmission with an empty carrier, condition (13) gives

$$r_T < \frac{\eta(\eta - 1)(W + 1)C}{2[(\eta - 1)(N_T + N_W) + \eta_{TW}rN_L]}. \quad (85)$$

For analysis of the ring/PSC stability condition (14), we fix the ring network to the structure illustrated in Fig. 2 with $N_r = 12$ ring nodes, $P = 4$ COs (of which $H = 1$ is a hotspot CO), and with three ring nodes between two COs. The highest traffic rate on a PSC channel arises for the uniform traffic pattern on the channel toward a CO with attached EPON when the hotspot CO is four ring hops from the considered CO. We refer henceforth to the considered CO as the “target CO”, the CO opposite of the target CO around the ring as the “opposite CO”, and the CO situated four hops along the ring from the target CO as the “adjacent CO” (which is located opposite the hotspot CO). We have the following contributions to the traffic load on the PSC home channel of the target CO:

- The opposite CO has $N_T + N_W$ TDM/WDM ONUs sending (*i*) to the N nodes in the EPON attached to the target CO, plus (*ii*) to the two ring nodes adjacent to the target CO, plus (*iii*) with probability one half to the two ring nodes situated two hops from the target CO over the target home channel. In addition, the opposite CO has N_L LR ONUs sending (*i*) to the $N_T + N_W$ TDM/WDM ONUs in the EPON attached to the target CO, plus (*ii*) to the two ring nodes adjacent to the target CO, plus (*iii*) with probability one half to the two ring nodes situated two hops from the target CO over the target channel. Thus, the opposite CO contributes

$$\frac{r_T}{\eta}(N_T + N_W)\frac{N + 2 + \frac{1}{2}2}{\eta - 1} + \frac{r_T}{\eta}N_L\frac{N_T + N_W + 2 + \frac{1}{2}2}{\eta - 1}. \quad (86)$$

- The adjacent CO has the same contribution as the opposite CO, except that only the traffic to the two ring nodes adjacent to the target CO is sent over the PSC; the ring nodes situated two hops from the target CO are reached with two hops over the ring (versus three hops over the PSC and then ring). Furthermore, the hotspot contributes as much as one LR ONU at the adjacent CO. Overall, the contribution from the adjacent CO and hotspot is thus

$$\frac{r_T}{\eta}(N_T + N_W)\frac{N + 2}{\eta - 1} + \frac{r_T}{\eta}(N_L + 1)\frac{N_T + N_W + 2}{\eta - 1}. \quad (87)$$

- The four ring nodes situated within two ring hops from the target CO do not send traffic toward the target CO over the PSC.
- The two ring nodes situated three hops in either ring direction from the target CO send to all ONUs attached to the target CO over the PSC (and directly over the ring to the ring nodes one and two hops from the target CO) contributing

$$\frac{r_T}{\eta}2\frac{N}{\eta - 1}. \quad (88)$$

TABLE I
SUMMARY OF STABILITY CONDITIONS AND RESULTING LIMITS ON TOTAL TRAFFIC BIT RATE IN NETWORK r_T FOR
DIFFERENT UNIFORM SOURCE-UNIFORM DESTINATION TRAFFIC SCENARIOS

Cap. Const.	r_T lim.	$N_T = 32$	$N_T = 24, N_W = N_L = 4$	$N_T = 16, N_W = N_L = 8$	$N_T = 4, N_W = N_L = 14$
T,u (9)	(80)	3.41	4.54	6.81	27.25
W,u (10)	(82)	N/A	6.91	7.21	8.21
T,d (11)	(80)	3.41	4.54	6.81	27.25
W,d, refl. (12)	(82)	N/A	6.91	7.21	8.21
W,d, empty car. (13)	(85)	N/A	3.45	3.61	4.10
Ring/PSC (14)	(91)	4.69	4.75	4.95	5.59
AWG (15)	(92)	N/A	735.75	183.94	60.06

- The four ring nodes situated five or six hops in either ring direction from the target CO send to all ONUs attached to the target CO plus to the two ring nodes adjacent to the target CO over the PSC contributing

$$\frac{r_T}{\eta} 4 \frac{N+2}{\eta-1}. \quad (89)$$

- The two ring nodes situated seven hops in either ring direction from the target CO send to all ONUs attached to the target CO, plus to the two ring nodes adjacent to the target CO, plus with probability one half to the two ring nodes situated two hops from the target CO over the PSC contributing

$$\frac{r_T}{\eta} 2 \frac{N+2+\frac{1}{2}2}{\eta-1}. \quad (90)$$

Combining these contributions results in the constraint

$$r_T < \frac{\eta(\eta-1)C}{(N+3)(N_T+N_W+2) + (N+2)(N_T+N_W+4) + N_L(2N_T+2N_W+5) + 2N + N_T + N_W + 2}. \quad (91)$$

For the considered uniform traffic, the maximum $\lambda^A(k, l)$ arises for the AWG channel from a CO with an attached EPON to another CO with an attached EPON. Specifically, the tightest AWG constraint (15) becomes

$$r_T < \frac{\eta(\eta-1)cC}{N_L^2}. \quad (92)$$

B. Non-uniform Source-Uniform Destination Traffic In this section we consider non-uniform source traffic whereby nodes generate different traffic rates. However, we continue to consider uniform destination traffic, i.e., each generated packet is destined to any of the other $\eta-1$ nodes with equal probability. More specifically, N_m of the ONUs in each EPON, as well as all ring nodes generate a medium traffic bit rate $\sigma\bar{L}$. Furthermore, given a source traffic non-uniformity α , $\alpha \geq 1$, N_l ONUs in each EPON generate a low traffic bit rate $\sigma\bar{L}/\alpha$. Also, N_h ONUs in each EPON and the hotspot CO generate a high traffic bit rate $\alpha\sigma\bar{L}$. The total traffic bit rate in the network is

$$r_T = \left[(P-H) \left(\frac{N_l}{\alpha} + N_m + \alpha N_h \right) + N_r + \alpha H \right] \sigma\bar{L}. \quad (93)$$

For notational convenience, we define the equivalent number of medium bit rate traffic nodes as

$$\eta_\alpha = (P-H) \left(\frac{N_l}{\alpha} + N_m + \alpha N_h \right) + N_r + \alpha H, \quad (94)$$

with which we express the medium traffic bit rate in terms of r_T as $\sigma\bar{L} = r_T/\eta\alpha$. The traffic routing rules from the preceding section apply, that is, traffic is sent over the AWG whenever possible.

Initially, all ONUs are TDM ONUs. Then, the medium rate ONUs are upgraded to WDM ONUs and the high rate ONUs are upgraded to LR ONUs. For the scenario with only TDM ONUs, the upstream TDM EPON channel condition (9) gives $\lambda^{T,u,k} = \frac{r_T}{\eta\alpha} \cdot [\frac{N_l}{\alpha} + N_m + \alpha N_h]$, giving the stability condition in terms of r_T

$$r_T < \frac{\eta\alpha C}{\frac{N_l}{\alpha} + N_m + \alpha N_h}. \quad (95)$$

For the downstream TDM channel condition (11) in the initial (non-upgraded) scenario, there is a load contribution $\frac{r_T}{\eta\alpha} (\frac{N_l}{\alpha} + N_m + \alpha N_h) \frac{N-1}{\eta-1}$ due to the ONUs in the considered EPON sending to other ONUs in the same EPON, and a contribution $\frac{r_T}{\eta\alpha} [(P-H-1)(\frac{N_l}{\alpha} + N_m + \alpha N_h) + N_r + \alpha H] \frac{N}{\eta-1} = \frac{r_T}{\eta\alpha} [\eta\alpha - (\frac{N_l}{\alpha} + N_m + \alpha N_h)] \frac{N}{\eta-1}$ due to the other network nodes sending to the ONUs in the considered EPON, resulting in the limit

$$r_T < \frac{\eta\alpha(\eta-1)C}{\eta\alpha N - (\frac{N_l}{\alpha} + N_m + \alpha N_h)}. \quad (96)$$

For the PSC in the initial setting, we obtain following the analysis above the contributions:

- Opposite CO: $\frac{r_T}{\eta\alpha} (\frac{N_l}{\alpha} + N_m + \alpha N_h) \frac{N+2+\frac{1}{2}}{\eta-1}$
- Adjacent CO and hotspot: $\frac{r_T}{\eta\alpha} (\frac{N_l}{\alpha} + N_m + \alpha(N_h + 1)) \frac{N+2}{\eta-1}$
- Ring nodes three hops from target CO: $\frac{r_T}{\eta\alpha} 2 \frac{N}{\eta-1}$
- Ring nodes four and five hops from target CO: $\frac{r_T}{\eta\alpha} 4 \frac{N+2}{\eta-1}$
- Ring nodes six hops from target CO: $\frac{r_T}{\eta\alpha} 2 \frac{N+2+\frac{1}{2}}{\eta-1}$

The resulting stability limit is

$$r_T < \frac{\eta\alpha(\eta-1)C}{(\frac{N_l}{\alpha} + N_m + \alpha N_h)(2N+5) + 8N + 14 + \alpha(N+2)}. \quad (97)$$

Next, for the upgraded scenario, $N_T = N_l$, $N_W = N_m$, and $N_L = N_h$. For the upstream TDM channel,

$$r_T < \frac{\eta\alpha C}{\frac{N_l}{\alpha}}. \quad (98)$$

For the upstream WDM channels we obtain

$$\lambda^{W,u,k} = \frac{r_T}{\eta\alpha} \left(N_m + \alpha N_h \frac{\eta T W r}{\eta-1} \right) \quad (99)$$

and the corresponding limit

$$r_T < \frac{\eta\alpha(\eta-1)(W+1)C}{(\eta-1)(\frac{N_l}{\alpha} + N_m) + \eta T W r \alpha N_L}. \quad (100)$$

For the downstream TDM channel we obtain by considering the transmissions from the each of the N_l TDM ONUs in the considered EPON sending with bit rate $r_T/(\eta\alpha)$ and a packet being destined to the other $N_l - 1$ TDM ONUs in the EPON with probability $(N_l - 1)/(\eta - 1)$ the load contribution

$\frac{r_T}{\eta_\alpha} \frac{N_l}{\alpha} \frac{N_l-1}{\eta-1}$. Further, considering the transmissions from all other nodes generating the traffic bit rate $\frac{r_T}{\eta_\alpha} [(P-H) (\frac{N_l}{\alpha} + N_m + \alpha N_h) + N_r + \alpha H - \frac{N_l}{\alpha}] = \frac{r_T}{\eta_\alpha} [\eta_\alpha - \frac{N_l}{\alpha}]$ of which the fraction $N_l/(\eta-1)$ is destined to the TDM ONUs in the considered EPON. Hence,

$$\lambda^{T,d,k} = \frac{r_T}{\eta_\alpha} \left[\frac{N_l}{\alpha} \frac{N_l-1}{\eta-1} + \left(\eta_\alpha - \frac{N_l}{\alpha} \right) \frac{N_l}{\eta-1} \right], \quad (101)$$

resulting in the limit

$$r_T < \frac{\eta_\alpha(\eta-1)C}{\frac{N_l}{\alpha}(\alpha\eta_\alpha-1)}. \quad (102)$$

For the WDM downstream channels when using signal reflection for upstream transmissions, we denote for convenience

$$\eta_{TW r\alpha} = (P-H) \left(\frac{N_l}{\alpha} + N_m \right) + N_r \quad (103)$$

and obtain by considering (i) the transmissions from the N_m medium bit rate ONUs at the EPON to the other medium bit rates ONUs at the EPON, (ii) the transmissions by all other nodes in the networks to the medium bit rate ONUs in the EPON, and (iii) the transmissions by all TDM/WDM ONUs and ring nodes in the network to the high bit rate ONUs in the EPON

$$\lambda^{W,d,k} = \frac{r_T}{\eta_\alpha} \left[N_m \frac{N_m-1}{\eta-1} + (\eta_\alpha - N_m) \frac{N_m}{\eta-1} + \eta_{TW r\alpha} \frac{N_h}{\eta-1} \right], \quad (104)$$

resulting in the limit

$$r_T < \frac{\eta_\alpha(\eta-1)(W+1)C}{(\alpha\eta_\alpha-1) \frac{N_l}{\alpha} + (\eta_\alpha-1)N_m + \eta_{TW r\alpha}N_h}. \quad (105)$$

For the WDM downstream channels using an empty carrier for upstream transmissions, we obtain

$$r_T < \frac{\eta_\alpha(\eta-1)(W+1)C}{\eta_\alpha(\eta-1)N_l + (\eta_\alpha + \eta - 2)N_m + (\alpha\eta_{TW r} + \eta_{TW r\alpha})N_h}. \quad (106)$$

For the PSC, we have the contributions:

- Opposite CO: $\frac{r_T}{\eta_\alpha} \left(\frac{N_l}{\alpha} + N_m \right) \frac{N+3}{\eta-1} + \frac{r_T}{\eta_\alpha} \alpha N_h \frac{N_l+N_m+3}{\eta-1}$
- Adjacent CO and hotspot: $\frac{r_T}{\eta_\alpha} \left(\frac{N_l}{\alpha} + N_m \right) \frac{N+2}{\eta-1} + \frac{r_T}{\eta_\alpha} \alpha (N_h + 1) \frac{N_l+N_m+2}{\eta-1}$
- Ring nodes three hops from target CO: $\frac{r_T}{\eta_\alpha} 2 \frac{N}{\eta-1}$
- Ring nodes four and five hops from target CO: $\frac{r_T}{\eta_\alpha} 4 \frac{N+2}{\eta-1}$
- Ring nodes six hops from target CO: $\frac{r_T}{\eta_\alpha} 2 \frac{N+3}{\eta-1}$

The resulting stability limit is

$$r_T < \frac{\eta_\alpha(\eta-1)C}{(N+3) \left(\frac{N_l}{\alpha} + N_m + 2 \right) + (N+2) \left(\frac{N_l}{\alpha} + N_m + 4 \right) + \alpha N_h (2N_l + 2N_m + 5) + 2N + N_l + N_m + 2} \quad (107)$$

For the AWG we obtain the highest load $\frac{r_T}{\eta_\alpha} \alpha N_h \frac{N_h}{\eta-1}$ and the corresponding limit

$$r_T < \frac{\eta_\alpha(\eta-1)cC}{\alpha N_h^2}. \quad (108)$$

We initially consider $N_l = 16$, $N_m = 8$, $N_h = 8$ with $\alpha = 2$.

TABLE II
SUMMARY OF STABILITY CONDITIONS AND RESULTING LIMITS ON TOTAL TRAFFIC BIT RATE IN NETWORK r_T FOR DIFFERENT NONUNIFORM SOURCE-UNIFORM DESTINATION TRAFFIC SCENARIOS FOR THE TDM ONUS-ONLY (NON-UPGRADED NETWORK AND THE UPGRADED NETWORK)

Cap. Const.	r_T lim.	
	TDM ONUs only	
T,u (9)	(95)	3.44
T,d (11)	(96)	3.41
Ring/PSC (14)	(97)	4.67
	Upgraded Network	
T,u (9)	(98)	13.75
W,u (10)	(100)	7.73
T,d (11)	(102)	6.78
W,d, refl. (12)	(105)	7.65
W,d, empty car. (13)	(106)	0.12
Ring/PSC (14)	(107)	5.28
AWG (15)	(108)	92.81

C. Non-uniform Source-Non-uniform Destination Traffic In this section we further build on the non-uniform source traffic from the preceding section in that we introduce non-uniform destinations. Specifically, we denote

$$\eta_{LH} = (P - H)N_L + H \quad (109)$$

for the total number of LR ONUs and hotspots in the network. With non-uniform destination traffic, a packet generated at an LR ONU or hotspot CO is destined to another LR ONUs/hotspot CO with probability β , $(\eta_{LH} - 1)/(\eta - 1) \leq \beta \leq 1$. A packet that is destined to another LR ONUs/hotspot CO is destined to any of the $\eta_{LH} - 1$ other LR ONUs/hotspot COs with equal probability. Packets generated at ring nodes, WDM or TDM ONUs are destined to any of the other network nodes with equal probability. We consider in the following the upgraded network scenario with $N_T = N_l$, $N_W = N_m$, and $N_L = N_h$. The upstream TDM channel carries only traffic from the TDM nodes, and is therefore not affected by the non-uniformity of the traffic destinations. Hence, the condition (98) still holds.

For the upstream WDM channels, we note that an LR ONU sends a packet with probability $1 - \beta$ over the upstream WDM channels. Hence,

$$\lambda^{W,u,k} = \frac{r_T}{\eta_\alpha} [N_m + \alpha N_h(1 - \beta)] \quad (110)$$

and

$$r_T < \frac{\eta_\alpha(W + 1)C}{\frac{N_l}{\alpha} + N_m + \alpha N_h(1 - \beta)}. \quad (111)$$

For the downstream TDM channel, the TDM ONUs at the considered EPON make the load contribution $\frac{r_T}{\eta_\alpha} \frac{N_l}{\alpha} \frac{N_l - 1}{\eta - 1}$, as above for the analysis leading to (102). All other TDM ONUs together with all WDM ONUs and ring nodes make the contribution $\frac{r_T}{\eta_\alpha} [(P - H) (\frac{N_l}{\alpha} + N_m) + N_r - \frac{N_l}{\alpha}] \frac{N_l}{\eta - 1} = \frac{r_T}{\eta_\alpha} [\eta_{TW} r_\alpha - \frac{N_l}{\alpha}] \frac{N_l}{\eta - 1}$. Furthermore, the LR ONUs and hotspots make the contribution $\frac{r_T}{\eta_\alpha} ((P - H)\alpha N_h + \alpha H) (1 - \beta) \frac{N_l}{\eta_{TW} r}$ =

$\frac{r_T}{\eta_\alpha} \alpha \eta_{LH} (1 - \beta) \frac{N_l}{\eta_{TW_r}}$, resulting in

$$\lambda^{T,d,k} = \frac{r_T N_l}{\eta_\alpha} \left[\frac{1}{\eta - 1} \left(\eta_{TW_r \alpha} - \frac{1}{\alpha} \right) + \frac{\alpha(1 - \beta)}{\eta_{TW_r}} \eta_{LH} \right], \quad (112)$$

and the limit

$$r_T < \frac{\eta_\alpha C}{N_l \left\{ \frac{1}{\eta - 1} \left(\eta_{TW_r \alpha} - \frac{1}{\alpha} \right) + \frac{\alpha(1 - \beta)}{\eta_{TW_r}} \eta_{LH} \right\}}. \quad (113)$$

For the WDM downstream channels when using signal reflection for upstream transmissions, traffic contributions are made by (i) the transmissions from the N_m medium bit rate ONUs at the EPON to the other medium bit rates ONUs at the EPON, (ii) the transmissions by all other TDM/WDM ONUs and ring nodes in the networks to the medium bit rate ONUs in the EPON, (iii) the transmissions by the LR ONUs and hotspots to the medium bit rate ONUs in the EPON, and (iv) the transmissions by all TDM/WDM ONUs and ring nodes in the network to the high bit rate ONUs in the EPON

$$\lambda^{W,d,k} = \frac{r_T}{\eta_\alpha} \left[\frac{N_m}{\eta - 1} (\eta_{TW_r \alpha} - 1) + \alpha(1 - \beta) \eta_{LH} \frac{N_m}{\eta_{TW_r}} + \eta_{TW_r \alpha} \frac{N_h}{\eta - 1} \right], \quad (114)$$

resulting in the limit

$$r_T < \frac{\eta_\alpha (W + 1) C}{(\eta_{TW_r \alpha} - 1) \frac{N_m}{\eta - 1} + \alpha(1 - \beta) \eta_{LH} \frac{N_m}{\eta_{TW_r}} + \eta_{TW_r \alpha} \frac{N_h}{\eta - 1}}. \quad (115)$$

For the WDM downstream channels using an empty carrier for upstream transmissions, we obtain

$$r_T < \frac{\eta_\alpha (W + 1) C}{\frac{N_l}{\alpha} + N_m + \alpha(1 - \beta) N_h + \frac{N_l}{\eta - 1} \left(\eta_{TW_r \alpha} - \frac{1}{\alpha} \right) + \frac{N_m}{\eta - 1} (\eta_{TW_r \alpha} - 1) + \frac{\alpha(1 - \beta) \eta_{LH}}{\eta_{TW_r}} (N_l + N_m) + \eta_{TW_r \alpha} \frac{N_h}{\eta - 1}} \quad (116)$$

For the PSC, we have the contributions:

- Opposite CO: $\frac{r_T}{\eta_\alpha} \left(\frac{N_l}{\alpha} + N_m \right) \frac{N+3}{\eta-1} + \frac{r_T}{\eta_\alpha} \alpha N_h (1 - \beta) \frac{N_l + N_m + 3}{\eta_{TW_r}}$
- Adjacent CO and hotspot: $\frac{r_T}{\eta_\alpha} \left(\frac{N_l}{\alpha} + N_m \right) \frac{N+2}{\eta-1} + \frac{r_T}{\eta_\alpha} \alpha (N_h + 1) (1 - \beta) \frac{N_l + N_m + 2}{\eta_{TW_r}}$
- Ring nodes three hops from target CO: $\frac{r_T}{\eta_\alpha} 2 \frac{N}{\eta-1}$
- Ring nodes four and five hops from target CO: $\frac{r_T}{\eta_\alpha} 4 \frac{N+2}{\eta-1}$
- Ring nodes six hops from target CO: $\frac{r_T}{\eta_\alpha} 2 \frac{N+3}{\eta-1}$

The resulting stability limit is

$$r_T < \frac{\eta_\alpha C}{\frac{1}{\eta-1} \left[\left(\frac{N_l}{\alpha} + N_m \right) (2N + 5) + (8N + 14) \right] + \frac{\alpha(1-\beta)}{\eta_{TW_r}} [N_h (N_l + N_m + 3) + (N_h + 1) (N_l + N_m + 2)]} \quad (117)$$

For the AWG we obtain the highest load $\frac{r_T}{\eta_\alpha} \alpha N_h \beta \frac{N_h}{\eta_{LH}}$ and the corresponding limit

$$r_T < \frac{\eta_\alpha \eta_{LH} C}{\alpha \beta N_h^2}. \quad (118)$$

We initially consider $N_l = 16$, $N_m = 8$, $N_h = 8$ with $\alpha = 2$ and $\beta = 0.75$.

TABLE III
SUMMARY OF STABILITY CONDITIONS AND RESULTING LIMITS ON TOTAL TRAFFIC BIT RATE IN NETWORK r_T FOR
DIFFERENT NONUNIFORM SOURCE-NONUNIFORM DESTINATION TRAFFIC SCENARIOS)

Cap. Const.	r_T lim.	
T,u (9)	(98)	13.75
W,u (10)	(111)	11
T,d (11)	(113)	9.83
W,d, refl. (12)	(115)	21.99
W,d, empty car. (13)	(116)	5.34
Ring/PSC (14)	(117)	7.14
AWG (15)	(118)	28.65

A. Empty Carrier vs. Signal Reflection for WDM Channel Upstream Transmission

We initially consider the following elementary per-TDM cycle switching policy for switching between upstream and downstream transmission on the W^k WDM channels. For ease of exposition, we explain the policy first for $W^k = 1$ channel. During a given cycle on the TDM channel, the OLT collects (a) both the REPORT messages (upstream transmission requests) from the attached ONUs as well as (b) the packets arriving at the OLT for forwarding downstream on the WDM channels to the ONUs. At the end of the cycle, i.e., when REPORT messages from all attached ONUs have been received, the OLT schedules: (a) All the requested upstream transmissions to arrive contiguously (spaced by appropriate guard intervals) at the OLT. We initially consider Gated service whereby the full upstream transmission request is granted and schedule the upstream grants in a first-come-first-served manner. At the end of the upstream transmissions, a switch over is scheduled. (b) After the switchover, the OLT schedules the transmission of all the downstream packets collected in the cycle in first-come-first-served manner, followed by a switchover. With this per-TDM cycle switching policy the OLT schedules two switchovers corresponding to each TDM cycle. Scheduling takes place at the end of every cycle on the TDM channel, i.e., when again REPORTs from all ONUs have been received. Note that the length of the upstream plus downstream transmission schedule on the WDM channel is not necessarily equal to the length of the cycle on the TDM channel. If a large upstream traffic volume is reported and a large downstream traffic volume collected the OLT may schedule the upstream and downstream transmissions way into the future. However, to every cycle on the TDM channel there corresponds one upstream-plus-downstream transmission schedule on the WDM channel.

We extend the outlined per-TDM cycle scheduling policy for $W^k = 1$ WDM channel to $W^k > 1$ WDM channels as follows. As with $W^k = 1$, the OLT schedules the upstream and downstream transmissions once per TDM cycle. The computed upstream plus downstream schedule is assigned to the W^k channels in round-robin fashion. That is, a given WDM channel is assigned a schedule every W^k cycles on the TDM channel.

REFERENCES

- [1] F. Effenberger, D. Clearly, O. Haran, G. Kramer, R. D. Li, M. Oron, and T. Pfeiffer, "An introduction to PON technologies," *IEEE Communications Magazine*, vol. 45, no. 3, pp. S17–S25, Mar. 2007.
- [2] L. G. Kazovsky, W.-T. Shaw, D. Gutierrez, N. Cheng, and S.-W. Wong, "Next-generation optical access networks," *IEEE/OSA J. of Lightwave Tech.*, vol. 25, no. 11, pp. 3428–3442, Nov. 2007.
- [3] J. Zhang, N. Ansari, Y. Luo, F. Effenberger, and F. Ye, "Next-generation PONs: A performance investigation of candidate architectures for next-generation access stage 1," *IEEE Communications Magazine*, vol. 47, no. 8, pp. 49–57, Aug. 2009.
- [4] R. Lin, "Next generation PON in emerging networks," in *Proc. OFC/NFOEC*, San Diego, CA, Feb. 2008.
- [5] K. Grobe and J.-P. Elbers, "PON in adolescence: From TDMA to WDM-PON," *IEEE Communications Mag.*, vol. 46, no. 1, pp. 26–34, Jan. 2008.
- [6] G. Kramer, B. Mukherjee, and G. Pesavento, "IPACT: A dynamic protocol for an Ethernet PON (EPON)," *IEEE Communications Magazine*, vol. 40, no. 2, pp. 74–80, February 2002.
- [7] C. Assi, Y. Ye, S. Dixit, and M. Ali, "Dynamic bandwidth allocation for Quality-of-Service over Ethernet PONs," *IEEE Journal on Selected Areas in Communications*, vol. 21, no. 9, pp. 1467–1477, November 2003.
- [8] M. Ma, Y. Zhu, and T. Cheng, "A bandwidth guaranteed polling MAC protocol for Ethernet passive optical networks," in *Proceedings of IEEE INFOCOM*, vol. 1, March 2003, pp. 22–31, San Francisco, CA.
- [9] H. Naser and H. Mouftah, "A joint-ONU interval-based dynamic scheduling algorithm for ethernet passive optical networks," *IEEE/ACM Transactions on Networking*, vol. 14, no. 4, pp. 889–899, August 2006.
- [10] J. Zheng and H. Mouftah, "A survey of dynamic bandwidth allocation algorithms for Ethernet Passive Optical Networks," *Optical Switching and Networking*, vol. 6, no. 3, pp. 151–162, Jul. 2009.
- [11] H. Takagi, *Analysis of Polling Systems*. MIT Press, 1986.
- [12] C. G. Park, D. H. Han, and K. W. Rim, "Packet delay analysis of symmetric gated polling system for DBA scheme in an EPON," *Telecommunication Systems*, vol. 30, no. 1-3, pp. 13–34, Nov. 2005.
- [13] T. Holmberg, "Analysis of EPONs under the static priority scheduling scheme with fixed transmission times," in *Proceedings of IEEE Conference on Next Generation Internet Design and Engineering (NGI)*, Apr. 2006, pp. 192–199.
- [14] B. Lannoo, L. Verslegers, D. Colle, M. Pickavet, M. Gagnaire, and P. Demeester, "Analytical model for the IPACT dynamic bandwidth allocation algorithm in EPONs," *OSA Journal of Optical Networking*, vol. 6, no. 6, pp. 677–688, Jun. 2007.
- [15] F. Aurzada, M. Scheutzow, M. Herzog, M. Maier, and M. Reisslein, "Delay analysis of Ethernet Passive Optical Networks with gated service," *OSA Journal of Optical Networking*, vol. 7, no. 1, pp. 25–41, Jan. 2008.
- [16] X. Bai, A. Shami, and Y. Ye, "Delay analysis of Ethernet passive optical networks with quasi-leaved polling and gated service scheme," in *Proc. of Second Int. Conference on Access Networks*, 2007, pp. 1–8.
- [17] S. Bharati and P. Saengudomlert, "Packet delay analysis for limited service bandwidth allocation algorithm in EPONs," in *Proc. First Asian Himalayas International Conference on Internet (AH-ICI)*, 2009, pp. 1–5.
- [18] S. Bhatia, D. Garbuzov, and R. Bartos, "Analysis of the Gated IPACT Scheme for EPONs," in *Proceedings of IEEE ICC*, Jun. 2006, pp. 2693–2698.
- [19] M. T. Ngo, A. Gravey, and D. Bhaduria, "A mean value analysis approach for evaluating the performance of EPON with Gated IPACT," in *Proc. of Int. Conference on Optical Network Design and Modeling (ONDM)*, 2008, pp. 1–6.
- [20] J. Vardakas and M. Logothetis, "Packet delay analysis for priority-based passive optical networks," in *Proceedings of Int. Conf. on Emerging Network Intelligence*, Oct. 2009, pp. 103–107.
- [21] Y. Luo and N. Ansari, "Dynamic upstream bandwidth allocation over Ethernet PONs," in *Proceedings of IEEE ICC*, May 2005, pp. 1853–1857.
- [22] Y. Zhu and M. Ma, "IPACT with grant estimation (IPACT-GE) scheme for Ethernet passive optical networks," *IEEE/OSA Journal of Lightwave Technology*, vol. 26, no. 14, pp. 2055–2063, Jul. 2008.
- [23] J. Vardakas, V. Vassilakis, and M. Logothetis, "Blocking analysis for priority classes in hybrid WDM-OCDMA passive optical networks," in *Proc. of Fifth Advanced International Conference on Telecommunications (AICT)*, 2009, pp. 389–394.
- [24] W.-R. Chang, "Research and design of system architectures and communication protocols for next-generation optical networks," Ph.D. dissertation, National Cheng Kung University, Tainan, Taiwan, 2008.
- [25] F. Aurzada, M. Scheutzow, M. Reisslein, and M. Maier, "Towards a fundamental understanding of the stability and delay of offline WDM EPONs," *IEEE/OSA Journal of Optical Communications and Networking*, vol. 2, no. 1, pp. 51–66, Jan. 2010.
- [26] J. Cai, A. Fumagalli, and I. Chlamtac, "The Multitoken Interarrival Time (MTIT) Access Protocol for Supporting Variable Size Packets Over WDM Ring Network," *IEEE Journal on Selected Areas in Communications*, vol. 18, no. 10, pp. 2094–2104, Oct. 2000.
- [27] M. A. Marsan, A. Bianco, E. Leonardi, M. Meo, and F. Neri, "On the Capacity of MAC Protocols for All-Optical WDM Multi-Rings with Tunable Transmitters and Fixed Receivers," in *Proc., IEEE INFOCOM*, vol. 3, Mar. 1996, pp. 1206–1216.
- [28] M. A. Marsan, E. Leonardi, M. Meo, and F. Neri, "Modeling slotted WDM rings with discrete-time Markovian models," *Computer Networks*, vol. 32, no. 5, pp. 599–615, May 2000.
- [29] I. Rubin and H.-T. Wu, "Performance analysis and design of CQBT algorithm for a ring network with spatial reuse," *IEEE/ACM Transactions on Networking*, vol. 4, no. 4, pp. 649–659, Aug. 1996.
- [30] F. Davik and S. Gjessing, "The Stability of the Resilient Packet Ring Aggressive Fairness Algorithm," in *Proc., IEEE LANMAN*, Apr. 2004, pp. 17–22.

- [31] V. Gambiroza, P. Yuan, L. Balzano, Y. Liu, S. Sheafor, and E. Knightly, "Design, Analysis, and Implementation of DVSR: A Fair High-Performance Protocol for Packet Rings," *IEEE/ACM Transactions on Networking*, vol. 12, no. 1, pp. 85–102, Feb. 2004.
- [32] I. Rubin and H.-K. H. Hua, "Synthesis and Throughput Behavior of WDM Meshed-Ring Networks Under Nonuniform Traffic Loading," *IEEE/OSA Journal of Lightwave Technology*, vol. 15, no. 8, pp. 1513–1521, Aug. 1997.
- [33] N. Mehravari, "Performance and protocol improvements for very high speed optical fiber local area networks using a passive star topology," *IEEE/OSA Journal of Lightwave Technology*, vol. 8, no. 4, pp. 520–530, Apr. 1990.
- [34] N. P. Caponio, A. M. Hill, F. Neri, and R. Sabella, "Single-layer optical platform based on WDM/TDM multiple access for large-scale 'switchless' networks," *European Trans. on Telecomm.*, vol. 11, no. 1, pp. 73–82, Jan./Feb. 2000.
- [35] C.-H. Chang, P. Kourtessis, and J. M. Senior, "GPON service level agreement based dynamic bandwidth assignment protocol," *IEE Electronics Letters*, vol. 42, no. 20, pp. 1173–1174, Sep. 2006.
- [36] J. Jiang, M. R. Handley, and J. M. Senior, "Dynamic bandwidth assignment MAC protocol for differentiated services over GPON," *IEE Electronics Letters*, vol. 42, no. 11, pp. 653–655, May 2006.
- [37] J. Jiang and J. Senior, "A new efficient dynamic MAC protocol for the delivery of multiple services over GPON," *Photonic Network Communications*, vol. 18, no. 2, pp. 227–236, Oct. 2009.
- [38] M. Hajduczenia, H. J. A. da Silva, and P. P. Monteiro, "EPON versus APON and GPON: a detailed performance comparison," *OSA Journal of Optical Networking*, vol. 5, no. 4, pp. 298–319, Apr. 2006.
- [39] B. Skubic, J. Chen, J. Ahmed, L. Wosinska, and B. Mukherjee, "A comparison of dynamic bandwidth allocation for EPON, GPON, and next-generation TDM PON," *IEEE Communications Magazine*, vol. 47, no. 3, pp. S40–S48, Mar. 2009.
- [40] M. McGarry, M. Maier, and M. Reisslein, "WDM Ethernet passive optical networks," *IEEE Comm. Mag.*, vol. 44, no. 2, pp. S18–S25, Feb. 2006.
- [41] R. Davey, D. Grossman, M. Rasztoivits-Wiech, D. Payne, D. Nettet, A. Kelly, A. Rafel, S. Appathurai, and S.-H. Yang, "Long-reach passive optical networks," *IEEE/OSA Journal of Lightwave Technology*, vol. 27, no. 3, pp. 273–291, Feb. 2009.
- [42] J. Lazaro, J. Prat, P. Chanclou, G. T. Beleffi, A. Teixeira, I. Tomkos, R. Soila, and V. Koratzinos, "Scalable extended reach PON," in *Proc. OFC*, Feb. 2008.
- [43] F. Saliou, P. Chanclou, F. Laurent, N. Genay, J. Lazaro, F. Bonada, and J. Prat, "Reach Extension Strategies for Passive Optical Networks," *IEEE/OSA Journal of Optical Communications and Networking*, vol. 1, no. 4, pp. C51–C60, Sep 2009.
- [44] D. Shea and J. Mitchell, "Architecture to integrate multiple PONs with long reach DWDM backhaul," *IEEE Journal on Selected Areas in Communications*, vol. 27, no. 2, pp. 126–133, Feb 2009.
- [45] G. Talli and P. D. Townsend, "Hybrid DWDM-TDM long-reach PON for next-generation optical access," *IEEE/OSA Journal of Lightwave Technology*, vol. 24, no. 7, pp. 2827–2834, Jul. 2006.
- [46] L. Meng, C. Assi, M. Maier, and A. Dhaini, "Resource management in STARGATE-based Ethernet passive optical networks (SG-EPONs)," in *Proc. IEEE ICC*, Dresden, Germany, Jun. 2009.
- [47] M. Maier, M. Herzog, M. Scheutzow, and M. Reisslein, "PROTECTORATION: A fast and efficient multiple-failure recovery technique for resilient packet ring (RPR) using dark fiber," *IEEE/OSA Journal of Lightwave Technology*, vol. 23, no. 10, pp. 2816–2838, Oct. 2005.
- [48] L. Kleinrock, *Queueing Systems: Volume I: Theory*. Wiley, 1975.
- [49] W. Bux and M. Schlatter, "An approximate method for the performance analysis of buffer insertion rings," *IEEE Transactions on Communications*, vol. COM-31, no. 1, pp. 50–55, Jan. 1983.